Rhodium Complexes Based on Phosphorus Diamide Ligands: Catalyst Structure versus Activity and Selectivity in the Hydroformylation of Alkenes

Saskia C. van der Slot,† Paul C. J. Kamer,† Piet W. N. M. van Leeuwen,*,† Jan Fraanje,† Kees Goubitz,† Martin Lutz,‡ and Anthony L. Spek‡

Institute of Molecular Chemistry, University of Amsterdam, Nieuwe Achtergracht 166, 1018 WV Amsterdam, The Netherlands, and Department of Crystal and Structural Chemistry, Utrecht University, Padualaan 8, 3584 CH Utrecht, The Netherlands

Received December 20, 1999

The rhodium-catalyzed hydroformylation reaction of 1-octene with phosphorus diamide ligands has been investigated. Four monodentate phosphorus diamide ligands and six bidentate phosphorus diamide ligands derived from a 1,3,5-trisubstituted biuret structure have been synthesized. These types of ligands combine steric bulk with π-acidity. The rhodium complexes formed under CO/H_2 have been characterized by high-pressure spectroscopic techniques. Spectroscopic experiments revealed that the monodentate ligands form mixtures of $HRhL_2(CO)_2$ and $HRhL(CO)_3$. The ratio $HRhL_2(CO)_2$:$HRhL(CO)_3$ depends on the ligand concentration and its bulkiness. The bidentate ligands form stable, well-defined catalysts with the structure $HRhL\cap L(CO)_2$ under hydroformylation conditions. Both monodentate and bidentate ligands have been tested in the hydroformylation reaction of 1-octene. The monodentate ligands form very active catalysts, but the linear-to-branched ratio of the product is low. The bidentate ligands show improved selectivity compared to the monodentate ligands and an activity that is only slightly lower.

Introduction

Since the first publications concerning hydroformylation using rhodium complexes, this reaction has been subject of numerous mechanistic studies.[1−12] An important aspect has been the unraveling of the structure of the resting state of the catalyst in order to understand the outcome of the overall catalytic reaction. Recently it has been shown that the geometry of the catalyst and the properties of the ligands coordinated to the metal center, especially the electronic and steric properties and the bite angle of bidentate ligands, have a large effect on the catalyst activity and selectivity.[13−16]

The steric properties of the ligand influence the catalyst activity and selectivity considerably. The results of van Leeuwen et al.[17,18] have shown that ligands with large cone angles[19] form catalysts having the structure $HRhL(CO)_3$, which are very active hydroformylation catalysts. The regioselectivity is low because only one bulky monodentate ligand coordinates to the rhodium center. An important steric property for bidentate ligands is the bite angle. The bite angle determines whether both phosphorus atoms of the bidentate ligand coordinate at equatorial positions of the trigonal bipyramid (ee) or at an equatorial and at an apical position (ea). Casey[13,15] studied the effect of the bite angle on the selectivity of the hydroformylation catalyst and found a correlation between the regioselectivity and the coordination mode of the bidentate ligand in the trigonal-bipyramidal structure. The studies of van Leeuwen et al.,[16] however, showed that the coordination mode of a bidentate ligand per se does not determine the regioselectivity, as both isomers (ee and ea) may form the same four-coordinate intermediate in the hydroformylation cycle. Furthermore, they found that the

* To whom correspondence should be addressed. E-mail: pwnm@anorg.chem.uva.nl.
† University of Amsterdam.
‡ Utrecht University.

(1) Bath, S. S.; Vaska, L. *J. Am. Chem. Soc.* **1963**, *85*, 3500.
(2) Osborn, J. A.; Wilkinson, G.; Young, J. F. *Chem. Commun.* **1965**, 17.
(3) Vaska, L. *J. Am. Chem. Soc.* **1966**, *88*, 4100.
(4) Evans, D.; Osborn, J. A.; Wilkinson, G. *J. Chem. Soc. A* **1968**, 3133.
(5) Yagupsky, G.; Brown, C. K.; Wilkinson, G. *J. Chem. Soc. A* **1970**, 1392.
(6) Brown, C. K.; Wilkinson, G. *J. Chem. Soc. A* **1970**, 2753.
(7) Unruh, J. D.; Christenson, J. R. *J. Mol. Catal.* **1982**, *14*, 19.
(8) Moasser, B.; Gladfelter, W. L.; Roe, D. C. *Organometallics* **1995**, 14, 3832.
(9) Schmid, R.; Herrmann, W. A.; Frenking, G. *Organometallics* **1997**, *16*, 701.
(10) van Rooy, A.; Kamer, P. C. J.; van Leeuwen, P. W. N. M. *J. Organomet. Chem.* **1997**, *535*, 201.
(11) Matsubara, T.; Koga, N.; Ding, Y.; Musaev, G.; Morokuma, K. *Organometallics* **1997**, *16*, 1065.
(12) Feng, J.; Garland, M. *Organometallics* **1999**, *18*, 417.
(13) Casey, C. P.; Whiteker, G. T.; Melville, M. G.; Petrovich, L. M.; Gavney, J. A., Jr.; Powell, D. R. *J. Am. Chem. Soc.* **1992**, *114*, 5535.
(14) Buisman, G. J. H.; van der Veen, L. A.; Klootwijk, A.; de Lange, W. G. J.; Kamer, P. C. J.; van Leeuwen, P. W. N. M.; Vogt, D. *Organometallics* **1997**, *16*, 2929.
(15) Casey, C. P.; Paulsen, E. L.; Beuttenmueller, E. W.; Proft, B. R.; Malter, B. A.; Powell, D. R. *J. Am. Chem. Soc.* **1999**, *121*, 63.
(16) van der Veen, L. A.; Boele, M. D. K.; Bregman, F. R.; Kamer, P. C. J.; van Leeuwen, P. W. N. M.; Goubitz, K.; Fraanje, J.; Schenk, H.; Bo, C. *J. Am. Chem. Soc.* **1998**, *120*, 11616.
(17) van Leeuwen, P. W. N. M.; Roobeek, C. F. *J. Organomet. Chem.* **1983**, *258*, 343.
(18) Jongsma, T.; Challa, G.; van Leeuwen, P. W. N. M. *J. Organomet. Chem.* **1991**, *421*, 121.
(19) Tolman, C. A. *Chem. Rev.* **1977**, *77*, 313.

10.1021/om9910120 CCC: $19.00
Publication on Web 05/23/2000

ligand basicity also contributes to the catalyst performance. Previous studies,[7,20] though neglecting bite angle effects, showed that ligands with electron-withdrawing groups lead to more active and selective catalysts.

In an extrapolation of the results of steric and electronic ligand effects, it seems attractive to design strongly π-accepting ligands that create steric hindrance close to the rhodium center. Here we report on several monodentate and bidentate phosphorus diamides as ligands in the rhodium-catalyzed hydroformylation of linear alkenes. These ligands create more steric bulk close to the phosphorus atom compared to the electron-withdrawing phosphites because of the higher degree of substitution at nitrogen compared to oxygen, while their χ values[21] can be in the same range as those of phosphites. This combination will result in crowded, electron-poor rhodium catalysts, which might influence both activity and regioselectivity of the hydroformylation reaction in a desired way. Several examples are known of phosphorus diamide ligands used in the hydroformylation reaction.[22−25] The results obtained with these ligands show improved activity compared to phosphine systems and improved selectivity compared to phosphite systems.

We synthesized a series of four monodentate phosphorus diamide ligands in order to investigate the performance of the corresponding catalyst systems in the hydroformylation reaction. The ligands are based on a 1,3,5-trisubstituted biuret structure.[26] The electron-withdrawing acyl substituent on the nitrogen atom stabilizes the phosphorus−nitrogen bond and increases the π-acidity of the ligand. The solution structures of the rhodium complexes formed under hydroformylation conditions were determined. The influence of the catalyst structure on the activity and selectivity in the hydroformylation reaction was investigated. As the selectivities of the systems containing monodentate ligands remained low, we synthesized a series of bidentate phosphorus diamide ligands to form well-defined catalyst systems, aiming at hydroformylation catalysts that combine regioselectivity with high activity.

Results and Discussion

Synthesis and Determination of Steric and Electronic Ligand Properties. The monodentate ligands **1a**,**c** (Chart 1) were prepared in a straightforward way by reaction of phenylphosphorus dichloride with N,N′,N″-trisubstituted biuret in the presence of a base. **1b**,**d** were synthesized in two steps by the reaction of phosphorus trichloride with N,N′,N″-trisubstituted biuret followed by the reaction with the corresponding alcohol in the presence of a base. The ligands **1a**−**d** could easily be purified by column chromatography. The ligands are remarkably stable toward water and oxygen.

Chart 1. Monodentate Biuret-Based Ligand Structures

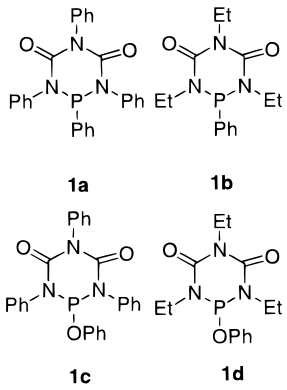

Chart 2. Bidentate Biuret-Based Ligand Structures

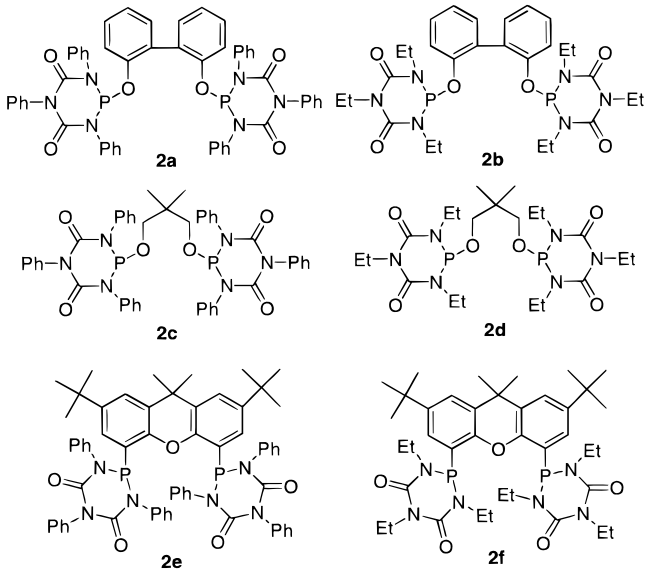

Table 1. Cone Angle θ Determined by the Use of Space-Filling Models

ligand	cone angle θ (deg)[a]
1a	189
1b	161
1c	148
1d	143

[a] See ref 19.

The bidentate ligands **2a**−**d** (Chart 2) were prepared by similar procedures from the chlorophosphorus diamide and the corresponding alcohol. Ligands **2e**,**f** were synthesized in a clean reaction from the dilithiated xanthene backbone and the corresponding chlorophosphorus diamide. No decomposition of the phosphorus−amide bond was observed in this reaction. Ligand **2c** was purified by washing with water. The bidentate ligands **2a**,**b**,**d**−**f** are not stable under these conditions, and therefore, they were purified by column chromatography.

The cone angles θ of the monodentate ligands **1a**−**d** were determined by the use of space filling models as described by Tolman.[19] Ligands **1a**−**d** have cone angles between 143 and 189° (Table 1). $\theta_{\mathbf{1a}}$ is larger than 180°. This indicates that there is space for only one ligand **1a** in the equatorial plane of a trigonal-bipyramidal

(20) Moser, W. R.; Papile, C. J.; Brannon, D. A.; Duwell, R. A. *J. Mol. Catal.* **1987**, *41*, 271.
(21) Tolman, C. A. *J. Am. Chem. Soc.* **1970**, *92*, 2953.
(22) van Rooy, A.; Burger, D.; Kamer, P. C. J.; van Leeuwen, P. W. N. M. *Recl. Trav. Chim. Pays-Bas* **1996**, *115*, 492.
(23) Trzeciak, A. M.; Glowiak, T.; Grybek, R.; Ziólkowski, J. *J. Chem. Soc., Dalton Trans.* **1997**, 1831.
(24) Breit, B. *J. Mol. Catal.* **1999**, *143*, 143.
(25) Naili, S.; Mortreux, A.; Agbossou, F. *Tetrahedron: Asymmetry* **1998**, 3421.
(26) Müller, C.; Meyer, T. G.; Farkens, M.; Sonnenburg, R.; Schmutzler, R. *Z. Naturforsch.* **1992**, *47B*, 760.

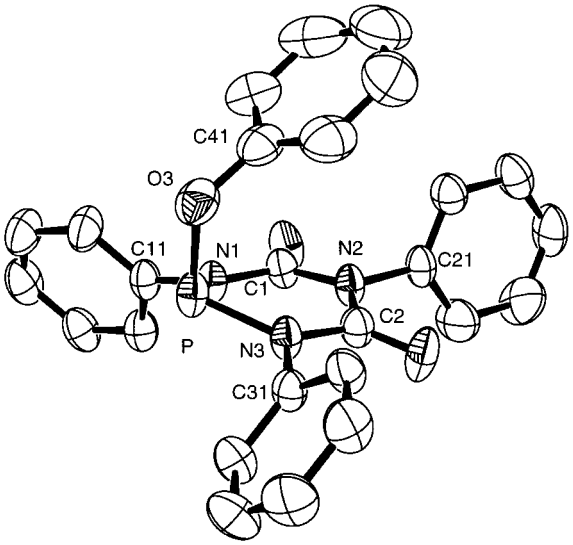

Figure 1. Displacement ellipsoid plot, plotted at the 50% probability level, of ligand **1c**.

Table 2. Selected Bond Distances (Å) and Bond Angles (deg) for 1c

Bond Distances			
P−N(1)	1.709(3)	N(1)−C(1)	1.388(4)
P−N(3)	1.720(3)	N(1)−C(11)	1.450(4)
P−O(3)	1.635(2)	N(3)−C(2)	1.386(4)
O(3)−C(41)	1.398(5)	N(3)−C(31)	1.446(4)
Bond Angles			
N(1)−P−N(3)	95.7(1)	O(3)−P−N(3)	104.3(1)
N(1)−P−O(3)	105.6(1)		

Table 3. Selected IR, NMR, and Crystal Structure Data of *trans*-RhCOClL_2 (L = 1a−d)

complex	ν_{CO} (cm^{-1})[a]	χ	J_{RhP} (Hz)	d_{Rh-P} (Å)
trans-RhClCO(PPh_3)$_2$[b]	1978	13	129	2.323(6)
trans-RhClCO(**1a**)$_2$ (**3a**)	2004		166	
trans-RhClCO(**1b**)$_2$ (**3b**)	2010		156	
trans-RhClCO(P(*o*-*t*-Bu-Ph)$_3$)$_2$[c]	2013	28	213	2.2856(7)
trans-RhClCO(P(OPh)$_3$)$_2$[b,d]	2016	29	217	
trans-RhClCO(**1c**)$_2$ (**3c**)	2021		212	2.2694(9) (P(1)) 2.3052(8) (P(2))
trans-RhClCO(**1d**)$_2$ (**3d**)	2025		209	2.279(1)

[a] Measured in CH_2Cl_2. [b] See ref 28. [c] See ref 26. [d] See ref 27.

structure. However, it must be taken into account that the substituents of the ligands can mesh into one another to achieve higher coordination numbers than expected. The crystal structure of **1c** (Figure 1, Table 2) shows that the higher degree of substitution at nitrogen compared to oxygen introduces steric hindrance close to the phosphorus atom.

The complexes *trans*-RhClCOL_2 (**3a**−**d**) were prepared to determine the electron-withdrawing character of ligands **1a**−**d**. Table 3 shows selected IR, NMR, and crystallographic data for **3a**−**d**. The crystal structures of **3c**,**d** are given in Figures 2 and 3, and selected bond distances and angles are given in Tables 4 and 5. Complex **3d** has a typical square-planar geometry with *cis*-L−Rh−L′ angles near 90° summing to 359°. Complex **3c** has a distorted-square-planar geometry with a *cis*-P(1)−Rh−Cl angle of 85.5(3)° and *cis*-P(2)−Rh−Cl angle of 84.8(3)°. The *cis*-P(1)−Rh−CO angle is 99.2(1)°, and the *cis*-P(2)−Rh−CO angle is 90.8(1)°. The angle sum at phosphorus atom P(1) (297.8°) is much smaller than the angle sums at P(2) (311.7°) and at the phosphorus

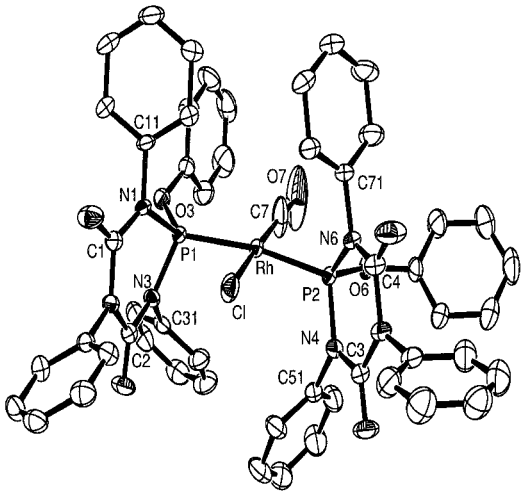

Figure 2. Displacement ellipsoid plot, plotted at the 50% probability level, of *trans*-RhClCO(**1c**)$_2$ (**3c**).

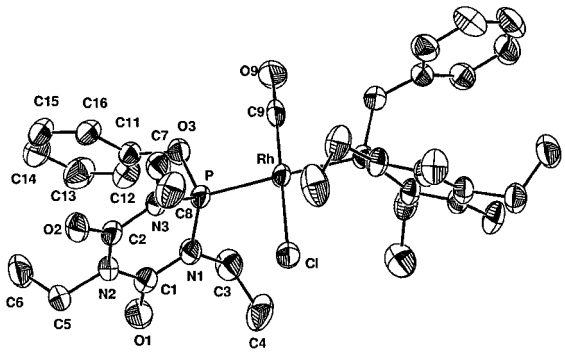

Figure 3. Displacement ellipsoid plot, plotted at the 50% probability level, of *trans*-RhClCO(**1d**)$_2$ (**3d**).

Table 4. Selected Bond Distances (Å) and Bond Angles (deg) for 3c

Bond Distances			
Rh−C(7)	1.820(5)	P(1)−O(3)	1.596(2)
Rh−P(1)	2.3052(8)	P(2)−N(4)	1.693(3)
Rh−P(2)	2.2694(9)	P(2)−N(6)	1.685(4)
Rh−Cl	2.3572(9)	C(7)−O(9)	1.136(6)
P(1)−N(1)	1.688(3)	P(2)−O(5)	1.604(3)
P(1)−N(3)	1.689(3)		
Bond Angles			
P(1)−Rh−Cl	85.49(3)	N(1)−P(1)−O(3)	100.2(1)
P(1)−Rh−C(7)	99.2(1)	N(1)−P(1)−N(3)	97.4(2)
P(1)−Rh−P(2)	169.19(3)	N(3)−P(1)−O(3)	100.2(1)
Cl−Rh−C(7)	174.4(2)	N(4)−P(2)−O(6)	106.4(2)
P(2)−Rh−C(7)	90.8(1)	N(4)−P(2)−N(6)	98.7(1)
Rh−C(7)−O(7)	175.3(4)	P(2)−N(6)−C(4)	129.5(3)
N(6)−P(2)−O(6)	106.6(1)	P(2)−N(6)−C(71)	116.1(1)
P(1)−N(1)−C(1)	126.9(3)	P(2)−N(4)−C(51)	116.0(2)
P(1)−N(1)−C(11)	115.9(2)	P(2)−N(4)−C(3)	128.6(3)
P(1)−N(3)−C(31)	115.9(2)	C(1)−N(1)−C(11)	116.7(3)
P(1)−N(3)−C(2)	125.3(3)	C(2)−N(3)−C(31)	116.9(3)
C(3)−N(4)−C(51)	115.2(3)	C(4)−N(6)−C(71)	114.1(3)

atom in the free ligand (305.6°). In the crystal structure, the phenoxy substituent has different conformations for P(1) and P(2), thereby influencing the angle sums at P(1) and P(2). In solution, free rotation around this bond will occur, and the resulting interchange between the two conformers leads to only one (averaged) signal for the two phosphorus atoms in the phosphorus NMR spectrum. The Rh−P(1) distance is in the same range as the Rh−P distances found in **3d** and RhClCO(P(*o*-*t*-

Table 5. Selected Bond Distances (Å) and Bond Angles (deg) for 3d

	Bond Distances		
Rh−C(9)	1.841(6)	P−N(1)	1.669(3)
Rh−P	2.279(1)	P−N(3)	1.680(3)
Rh−Cl	2.338(1)	P−O(3)	1.618(3)
C(9)−O(9)	1.142(7)		
	Bond Angles		
P−Rh−Cl	89.32(3)	N(1)−P−O(3)	106.6(2)
P−Rh−C(9)	90.68(3)	N(1)−P−N(3)	98.9(2)
P−Rh−P*	178.65(4)	N(3)−P−O(3)	105.6(1)
Cl−Rh−C(9)	180.00(0)	Rh−C(9)−O(9)	180.00(0)
P−N(1)−C(1)	127.2(3)	P−N(3)−C(2)	125.9(3)
C(3)−N(1)−C(1)	115.0(3)	C(7)−N(3)−C(2)	116.2(3)
C(3)−N(1)−P	116.2(3)	C(7)−N(3)−P	116.3(3)

Bu-C_6H_4)$_3$)$_2$.[27] The Rh−P(2) distance is longer than the Rh−P(1) distance. It seems that in the solid state the energetically most favored situation is to bend all substituents of P(2) away from the rhodium center. The phosphorus atom is positioned further away from the rhodium atom, thereby creating enough space for the substituents. The J_{RhP} (NMR) coupling constants of **3c**,**d** are in the same range as those of phosphite ligands, while the J_{RhP} coupling constants of **3a**,**b** are smaller.[27,28] Comparison of the IR frequencies of the carbonyl ligands of complexes **3a**−**d** and *trans*-RhClCO(PPh_3)$_2$, *trans*-RhClCO(P(OPh)$_3$)$_2$, and *trans*-RhClCO(P(*o*-*t*-Bu-C_6H_4)$_3$)$_2$ gives insight into the π-acidity of the ligands.[27,29] The ligands **1a**−**d** are stronger π-acids than triphenylphosphine. The carbonyl frequencies of **3a**−**d** indicate that **1a**,**b** are more basic than triphenyl phosphite and tris(*o*-*tert*-butylphenyl) phosphite, whereas **1c** and **1d** are better π-acids. Thus, the conclusion seems to be justified that the phosphorus diamide ligands derived from biuret are electronically similar to phosphite ligands, while the biuret group by itself is a better electron acceptor compared to two phenoxy groups. We expected the carbonyl frequencies of complexes **3a**,**c** to be higher than the carbonyl frequencies of complexes **3b**,**d**, respectively, based on the electron-withdrawing character of the phenyl substituents on the nitrogen atoms compared to the ethyl substituents. Probably the distortion in the complex has a larger influence on the carbonyl frequency of the carbonyl ligand than the influence of the electron-donating capacity of the substituents on the nitrogen atoms.

The bite angle is an important steric property for bidentate ligands. Previous research[30,31] showed that the backbones chosen for ligands **2a**−**f** seem to induce optimal bite angles for selective catalysis in the hydroformylation reaction. The bidentate ligands (**2a**−**f**) are based on the same phosphorus diamide structures as the monodentate ligands. The crystal structure of ligand **2a** (Figure 4, Table 6) shows that steric hindrance at the phosphorus atoms increases by the phenyl substituents on the nitrogen atoms. The huge steric bulk might

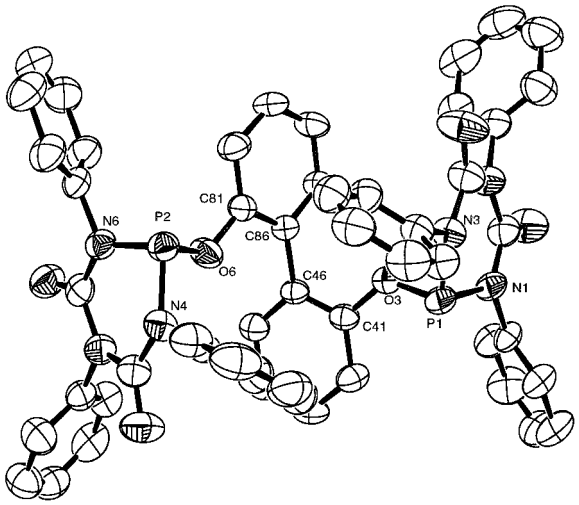

Figure 4. Displacement ellipsoid plot, plotted at the 50% probability level, of ligand **2a**.

Table 6. Selected Bond Distances (Å) and Bond Angles (deg) for 2a

	Bond Distances		
P(1)−N(1)	1.710(3)	P(2)−N(4)	1.703(4)
P(1)−N(3)	1.701(3)	P(2)−N(6)	1.698(4)
P(1)−O(3)	1.640(4)	P(2)−O(6)	1.647(3)
N(1)−C(11)	1.453(5)	N(4)−C(71)	1.459(6)
N(1)−C(1)	1.393(6)	N(4)−C(6)	1.393(5)
N(3)−C(31)	1.458(4)	N(5)−C(61)	1.446(5)
N(3)−C(2)	1.400(6)	N(5)−C(3)	1.384(7)
O(3)−C(41)	1.394(5)	O(6)−C(81)	1.398(5)
	Bond Angles		
N(1)−P(1)−O(3)	96.4(2)	N(4)−P(2)−O(6)	96.2(2)
N(1)−P(1)−N(3)	99.9(2)	N(4)−P(2)−N(6)	96.9(2)
N(3)−P(1)−O(3)	98.3(2)	N(6)−P(2)−O(6)	99.6(2)
P(2)−O(6)−C(81)	124.1(2)	P(1)−O(3)−C(41)	124.9(3)
C(81)−C(86)−C(46)	121.5(3)	C(86)−C(46)−C(45)	121.0(4)
C(85)−C(86)−C(46)	121.6(3)	C(41)−C(46)−C(86)	121.1(3)

even lead to monodentate behavior of **2a**. Ligands **2c,d** have very flexible backbones. The bidentate coordination mode creates steric hindrance close to both phosphorus atoms and the metal center. The electron-withdrawing character of ligands **2a**,**b** will be in the same range as that of ligands **1c**,**d** because of the similarity of the substituents on the phosphorus atom. Ligands **2a**,**b** will be more π-acidic relative to **2c**,**d** because of the more electron-withdrawing character of the aryl backbone compared to the alkyl backbone. The electronic character of ligands **2e**,**f** will be comparable to that of **1a**,**b**.

Catalyst Characterization Studies. The hydride formation under hydroformylation conditions was monitored using high-pressure (HP) NMR and HP IR spectroscopy in order to investigate the structures of these complexes. The hydride formation was studied using Rh(acac)(CO)$_2$ in the presence of various concentrations of ligand under 20 bar of CO/H_2 (1/1). Ligands **1a**,**b** gave complete conversion of Rh(acac)(CO)$_2$ to $HRhL_x(CO)_{4-x}$ (x = 1, 2) within 1 h at T = 80 °C. The hydride formation with ligands **1c**,**d** is very fast, as complete conversion of Rh(acac)(CO)$_2$ to $HRhL_x(CO)_{4-x}$ was reached within 1 h at T = 40 °C.

The spectroscopic data of the hydride complexes $HRhL_x(CO)_{4-x}$ (x = 1−3) with ligands **1a**−**d** are presented in Table 7. In all cases a mixture of $HRhL(CO)_3$ and $HRhL_2(CO)_2$ was observed. The ratio between $HRhL_2(CO)_2$ and $HRhL(CO)_3$ is dependent on the ligand

(27) Fernández, E.; Ruiz, A.; Claver, C.; Castillon, S. *Organometallics* **1998**, *17*, 2857.
(28) Li Wu, M.; Desmond, M. J.; Drago, R. S. *Inorg. Chem.* **1979**, *18*, 679.
(29) Haar, C. M.; Huang, J.; Nolan, S. P.; Petersen, J. L. *Organometallics* **1998**, *17*, 5018.
(30) van der Veen, L. A.; Kamer, P. C. J.; van Leeuwen, P. W. N. M. *Angew. Chem., Int. Ed.* **1999**, *38*, 336.
(31) van Rooy, A.; Kamer, P. C. J.; van Leeuwen, P. W. N. M.; Goubitz, K.; Fraanje, F.; Veldman, N.; Spek, A. L. *Organometallics* **1996**, *15*, 835.

Table 7. NMR and IR Data for $HRhL_x(CO)_{4-x}$ ($x = 1-3$) Complexes (L = 1a−d)

compd	$\delta(^{31}P)$ (ppm)[a]	J_{RhP} (Hz)	$\delta(^{1}H)$ (ppm)[a]	ν_{CO} (cm^{-1})[b]
HRh**1a**$(CO)_3$	110	186	−10.6 (d, $J_{PH} = 6$ Hz)	2094, 2047, 2017
HRh(**1a**)$_2(CO)_2$	114	196	−11.4 (t, $J_{PH} = 12$ Hz)	2079, 2023
HRh(**1b**)$(CO)_3$	104	177	−10.3 (d, $J_{PH} = 15$ Hz)	2095, 2045, 2008
HRh(**1b**)$_2(CO)_2$	110	181	−10.6 (s, br)	2070, 2018
HRh(**1b**)$_3$CO (**4**)	117	169	−10.7 (s, br)	2019
HRh(**1c**)$(CO)_3$	not obsd		not obsd	2096, 2047, 2020
HRh(**1c**)$_2(CO)_2$	126	221	−10.6 (s, br)	2071, 2003
HRh(**1d**)$(CO)_3$	116	220	not obsd	2098, 2043, 2014
HRh(**1d**)$_2(CO)_2$	118	224	−10.5 (s, br)	2076, 2020

[a] Measured in toluene-d_8. [b] Complexes with L = **1a**,**c** measured in 2-methyltetrahydrofuran; complexes with L = **1b**,**d** measured in cyclohexane.

concentrations as well as on the steric and electronic ligand properties. Lowering of the ligand and rhodium concentrations resulted in a decreasing amount of $HRhL_2(CO)_2$. The amount of $HRhL_2(CO)_2$ measured at the same ligand concentrations decreased in the order **1d** > **1c** > **1b** > **1a**. Rhodium complexes of the form $HRhL_x(CO)_{4-x}$ ($x = 1-3$) generally have a (distorted) trigonal-bipyramidal structure. Crystal structure analyses of transition-metal hydrides have shown that the hydride ligand coordinates at an apical position of the bipyramid.[32] The phosphorus atoms can coordinate either at the equatorial positions or at the remaining apical position. For transition-metal hydrides the absolute phosphorus−hydride (NMR) coupling constant is substantially larger for complexes having an HRhP angle approaching 180° than for those having angles of ∼90°.[33] Small *cis* J_{HP} values between 1 and 30 Hz are reported for hydride carbonyl complexes with bis equatorially coordinating diphosphine[16] and diphosphite ligands.[8] Larger phosphorus−hydride coupling constants in the range of 110−200 Hz are reported for axially coordinated phosphorus ligands.[33,34] HRh(**1a**)$(CO)_3$ and HRh(**1b**)$(CO)_3$ have phosphorus−hydride coupling constants of 6 and 15 Hz, respectively. This indicates that the phosphorus ligands coordinate in the equatorial plane of a slightly distorted trigonal bipyramid. The (IR) carbonyl frequencies of the complexes $HRhL(CO)_3$ (L = **1a**−**d**) are almost equal to the frequencies found for these types of complexes formed using bulky phosphites.[18]

The hydride complexes $HRhL_2(CO)_2$ (L = **1a**−**d**) have J_{PH} coupling constants of approximately 3−12 Hz, which is relatively large for a pure *cis* coordination. Two explanations can be brought forward. An equilibrium mixture of ee−ea coordination gives averaged signals in the NMR spectra, provided that there is a fast exchange of the phosphorus ligands between equatorial and apical positions.[35] Second, coordination of both phosphorus atoms in the equatorial plane of a slightly distorted trigonal bipyramid would lead to the same coupling constant. If an equilibrium between two isomers occurs, two sets of carbonyl frequencies are observed in the infrared spectra originating from the two isomers because of the faster time scale of this technique.[16] In general, the carbonyl bands of the ea isomer $HRhL_2(CO)_2$ are found at lower wavenumbers than those of the ee isomer. The infrared spectra showed that the hydride complexes $HRhL_2(CO)_2$ (L = **1a**−**d**) are present as only one isomer. The carbonyl frequencies indicate an ee coordination in a distorted-trigonal-bipyramidal structure, as confirmed by published carbonyl frequencies for bulky bidentate phosphite ligands.[31,34] HRh(**1a**)$_2(CO)_2$ was observed as the main complex in the high-pressure NMR experiments ([Rh] = 13 mM, [**1a**] = 0.13 M). This is very surprising in view of the large estimated cone angle ($\theta = 189°$). We therefor assume that the bulky moieties of the ligands are meshing or easily bent away.

The stability of the hydride complexes containing L = **1a**,**b** under 1 bar of CO/H_2 was investigated by NMR spectroscopy in the presence of an excess of ligand (Rh/L = 1/10). The pressure was released from the high-pressure NMR tube after the spectrum was recorded. The solution was transferred to a 5 mm NMR tube and measured again. We could see that the stability of the hydride complexes $HRhL_x(CO)_{4-x}$ depends on the ligand and the number of phosphorus ligands coordinated. $HRhL(CO)_3$ (L = **1a**,**b**) was never observed at atmospheric pressure in the presence of an excess of ligand. In this case a phosphorus ligand replaces a carbonyl ligand to form $HRhL_2(CO)_2$. HRh(**1a**)$_2(CO)_2$ is not stable for a longer period of time in the absence of CO/H_2 pressure, and the complex was observed in low concentrations only. The major part of the rhodium complex disproportionate, forming rhodium carbonyl clusters. HRh(**1b**)$_2(CO)_2$ was formed quantitatively from the mixture of **1b**, HRh(**1b**)$_2(CO)_2$, and HRh(**1b**)$(CO)_3$ when the same procedure was followed as for ligand **1a**. This complex is relatively stable in the absence of CO/H_2 pressure but converts slowly to HRh(**1b**)$_3$CO (**4**), which was analyzed by a crystal structure determination. The structure of complex **4** (Figure 5, Table 8) reveals a slightly distorted trigonal bipyramidal geometry, the three phosphorus ligands occupying equatorial positions. The structure has a crystallographic 3-fold axis along the Rh−CO bond. The rhodium atom is located slightly under the equatorial plane defined by the phosphorus atoms, displaced toward the carbonyl ligand. The hydrogen atom could not be located in the crystal structure, but ^1H NMR spectroscopy indicates that the hydride occupies the apical position of the trigonal bipyramid.

The hydride complexes HRh(**1c**)$_x(CO)_{4-x}$ and HRh(**1d**)$_x(CO)_{4-x}$ ($x = 1, 2$) decomposed when the temperature

(32) Frenz, B. A.; Ibers, J. A. *The Hydride Series*; Muetterties, E. L., Ed.; Marcel Dekker: New York, 1971; Vol. I, Chapter III.
(33) Nozaki, K.; Sakai, N.; Nanno, T.; Higashijima, T.; Mano, S.; Horiuchi, T.; Takaya, H. *J. Am. Chem. Soc.* **1997**, *119*, 4413.
(34) Buisman, G. J. H.; Vos, E. J.; Kamer, P. C. J.; van Leeuwen, P. W. N. M. *J. Chem. Soc., Dalton Trans.* **1995**, 409.
(35) Brown, J. M.; Kent, A. G. *J. Chem. Soc., Perkin Trans. 2* **1987**, 1597.

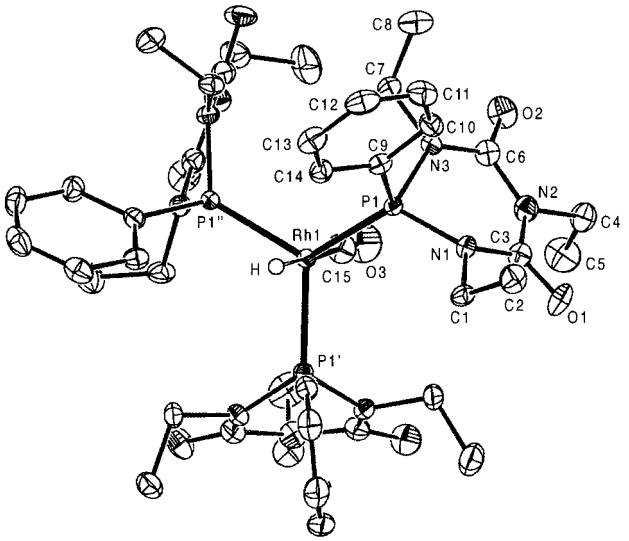

Figure 5. Displacement ellipsoid plot, plotted at the 50% probability level, of HRh(**1b**)$_3$CO (**4**).

Table 8. Selected Bond Distances (Å) and Bond Angles (deg) for 4

	Bond Distances		
Rh−C(15)	1.907(6)	P(1)−N(1)	1.721(3)
C(15)−O(3)	1.141(9)	P(1)−C(9)	1.827(4)
Rh−P(1)	2.2872(9)	P(1)−N(3)	1.718(4)
	Bond Angles		
P(1)−Rh−P(1′)	119.13(10)	P(1)−Rh−C(15)	95.38(3)
C(15)−Rh−H	180.0	N(3)−P(1)−C(9)	101.06(17)
Rh−P(1)−N(1)	121.90(12)	N(1)−P(1)−N(3)	95.10(15)
Rh−P(1)−N(3)	115.20(12)	C(9)−P(1)−N(1)	98.92(16)
Rh−P(1)−C(9)	120.02(13)		

was raised to 80 °C. HRh(**1c**)$_x$(CO)$_{4-x}$ converts within 1 h completely to [Rh$_4$(CO)$_{12}$] (ν_{CO} 2074 (s), 2068 (s), 2043 (m), 1885 cm^{-1} (m), with 2-methyltetrahydrofuran as solvent),[36] and this rhodium carbonyl cluster decomposes subsequently to form [Rh$_6$(CO)$_{16}$] at 80 °C (ν_{CO} 2074 (s), 1820 (s), with 2-methyltetrahydrofuran as solvent).[36] The hydride complexes of **1d** disproportionate to form a new hydride complex. We studied the decomposition of HRh(**1d**)$_x$(CO)$_{4-x}$ using HP NMR and HP IR spectroscopy. The phosphorus signals in the ^{31}P NMR spectrum belonging to the hydride complexes HRh(**1d**)$_x$(CO)$_{4-x}$ disappear when the solution is heated to 80 °C, and a new multiplet appears at δ 262 ppm. Additionally, a double triplet appears in the hydride region of the ^{1}H NMR spectrum (δ −10.7 ppm, J_{PH} = 18 Hz, J_{RhH} = 14 Hz in toluene-d_8). The ^{1}H−^{31}P COSY NMR spectrum shows only one correlation between this hydride signal and the phosphorus signal at 262 ppm. The hydride signal became a triplet when we decoupled the phosphorus signal selectively at 262 ppm. This indicates that we are dealing with a dimeric rhodium complex in which, surprisingly, one phosphorus atom is coordinated to two rhodium atoms. The low-field resonance of the phosphorus signal is strongly indicative of a phosphido group that bridges a metal−metal bond.[37,38]

The IR spectrum of the complex shows two carbonyl bands at 2041 (m) and 2003 cm^{-1} (m), indicating terminal positions. No bridging carbonyl bands were observed. The structure consistent with all data is depicted in Figure 6. The formation of phosphido type complexes is not uncommon in these systems.[39] Attempts to isolate this complex were not successful.

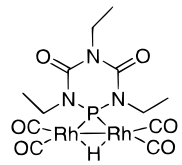

Figure 6. Proposed decomposition product of HRh(**1d**)$_x$(CO)$_{4-x}$.

Table 9. NMR and IR Data of HRhL(CO)$_2$ (L = 2a−d,f)

compd	δ(^{31}P)[a] (ppm)	J_{RhP} (Hz)	J_{PP} (Hz)	δ(^{1}H) (ppm)	ν_{CO} (cm^{-1})[b]
HRh(**2a**)(CO)$_2$	140[c]	244	211	−12.0 (t, J_{RhH} = 12 Hz)[c]	2085, 2041
	143[c]	251			
HRh(**2b**)(CO)$_2$	141	218		−11.1 (s, br)	2070, 2019
HRh(**2c**)(CO)$_2$	145	225	190	−11.7 (s, br)	2086, 2031
	147	226			
HRh(**2d**)(CO)$_2$	145	221		−10.6 (s, br)	2067, 2017
HRh(**2f**)(CO)$_2$	96	185		−10.2 (dt, J_{PH} = 17 Hz, J_{RhH} = 2 Hz)	2057, 2004

[a] Measured in toluene-d_8. [b] Complexes with L = **2a**,**c** measured in 2-methyltetrahydrofuran; complexes with L = **2b**,**d**,**f** measured in cyclohexane. [c] Measured in CD_2Cl_2.

The hydride formation for the bidentate ligands **2a**−**f** was studied using Rh(acac)(CO)$_2$ in the presence of 2 equiv (HP NMR) or 5 equiv (HP IR) of ligand under 20 bar of CO/H$_2$ (1/1). Ligands **2a**−**d**,**f** gave complete conversion of Rh(acac)(CO)$_2$ to HRhL∩L(CO)$_2$ within 1 h at 80 °C. In contrast to the complexes of the monodentate ligands, decomposition was observed for neither the hydride complexes nor the ligands. Ligand **2e** did not coordinate to rhodium at all. [Rh$_6$(CO)$_{16}$] is formed when a mixture of Rh(acac)(CO)$_2$ and **2e** under CO/H$_2$ is heated for 1 h at 80 °C. Probably, the ligand is too bulky to coordinate to the rhodium atom and Rh(acac)(CO)$_2$ is converted into the rhodium carbonyl cluster.

The spectroscopic data of the hydride complexes HRhL∩L(CO)$_2$ formed with ligands **2a**−**d**,**f** are presented in Table 9. The bidentate ligands form one single rhodium hydride complex, independent of the ligand concentration. The J_{RhP} coupling constants of the complexes HRhL(CO)$_2$ formed with L = **2a**−**d** are all in the same ranges as the J_{RhP} coupling constants found for the monodentate ligands **1c**,**d**, which indicates that the electronic character of these ligands is indeed comparable. The J_{RhP} coupling constant of HRh(**2f**)(CO)$_2$ is in the same range as the J_{RhP} coupling constants found for the monodentate ligands **1a** and **1b**. The hydride signals of the complexes formed with **2b**−**d** are broad singlets ($W_{1/2} \approx$ 10 Hz). This indicates that both J_{RhH} and J_{PH} coupling constants are small (<3 Hz). The small J_{PH} coupling constants are indicative of an ee coordination mode. The hydride signal of HRh(**2f**)(CO)$_2$ is a double triplet (J_{RhH} = 2 Hz, J_{PH} = 17 Hz). The J_{PH} coupling constant indicates ee coordination in a distorted trigonal bipyramid.

Even though ligand **2a** is very bulky, the ligand coordinates in a bidentate fashion. The two phosphorus atoms in HRh(**2a**)(CO)$_2$ are magnetically inequivalent

(36) Cattermole, P. E.; Osborne, A. G. *Inorg. Synth.* **1977**, *17*, 115.
(37) Arif, A. M.; Jones, R. A.; Seeberger, M. H.; Whittlesey, B. R.; Wright, T. C. *Inorg. Chem.* **1986**, *25*, 3943.
(38) Garrou, P. E. *Chem. Rev.* **1981**, *81*, 229.
(39) Sivak, A. J.; Muettterties, E. L. *J. Am. Chem. Soc.* **1979**, *101*, 4878.

Table 10. Hydroformylation Results of 1-Octene with L = 1a−d[a]

L	L/Rh	conversn (%)	l/b	TOF[b]	linear (%)	isomerizn[d] (%)
1a	50	30	2.6	24500	60	17
1b	50	33	2.3	10300	61	12
1c	100	34	2.3	7700[c]	56	19
1d	100	32	2.2	4920[c]	61	11

[a] Conditions: $T = 80$ °C, $p_{CO} = p_{H_2} = 10$ bar, [Rh] = 0.2 mM, [1-octene] = 0.64 M in toluene. [b] In units of (mol of aldehyde) (mol of Rh)$^{-1}$ h^{-1}. [c] Presuming that all rhodium added is active as a hydroformylation catalyst. [d] Formation of 2-octene.

and show a strongly coupled NMR spectrum. The small J_{PH} (<3 Hz) and the J_{RhP} coupling constant of 12 Hz in HRh(**2a**)$(CO)_2$ are in agreement with those of an ee coordination mode in a slightly distorted trigonal bipyramidal structure. The distortion in the complex is probably a result of the bulkiness of the ligand. In HRh(**2c**)$(CO)_2$ the phosphorus atoms lose their time-averaged equivalence on cooling from 80 °C to room temperature. At −25 °C the slow exchange region is reached, resulting in a strongly coupled NMR spectrum. The J_{PH} and J_{RhH} coupling constants remain small.

In the IR spectra only two carbonyl bands are observed. The positions of the carbonyl bands of the complexes containing ligands **2b**,**d**,**f** evidence an ee coordination of the bidentate ligands in a distorted trigonal bipyramid, in accordance with previous results.[14,16] The carbonyl frequencies of HRh(**2a**)$(CO)_2$ and HRh(**2c**)$(CO)_2$, however, shift to higher wavenumbers compared to those of hydride complexes containing **2b**,**d**,**f**, and the frequencies of the hydride complexes of the monodentate ligands. The crystal structure of **2a** (Figure 4) shows huge steric hindrance close to the phosphorus atoms due to the phenyl substituents on the nitrogen atoms. Coordination of the bidentate ligands **2a**,**c** to a metal center will increase this steric strain and distort the geometry of the trigonal bipyramid. This distortion does not seem to affect the phosphorus−hydride coupling constant. The distorted geometry may explain the difference in carbonyl frequencies of the hydride complexes of **2a**,**c** and the hydride complexes containing **2b**,**d**,**f**.

Hydroformylation of 1-Octene. The ligands **1a**−**d** were used in the rhodium-catalyzed hydroformylation of 1-octene. The catalysts were prepared in situ from Rh(acac)$(CO)_2$, the ligand, CO, and H_2 at 80 °C. In the previous section we have shown that two rhodium hydride complexes are formed, $HRhL(CO)_3$ and $HRhL_2(CO)_2$, depending on the ligand properties and the ligand and rhodium concentrations. The ligand and rhodium concentrations used in catalysis are much lower than the concentrations used in the spectroscopic experiments. Therefore, the proportion of $HRhL(CO)_3$ in the reaction mixture used in catalysis is assumed to be significantly higher than that in the spectroscopic experiments.

The results of the hydroformylation reaction of 1-octene obtained using L = **1a**−**d** are presented in Table 10. The very high activity of the catalysts formed is in the range of the activity of the bulky phosphite ligands studied by van Leeuwen et al.[40] They could show that the activity of these bulky phosphite systems increases with the electron-withdrawing character of the ligand. In the case of **1a**−**d**, the activity is determined predominantly by the type of complex rather than the ligand properties. A quantitative comparison of the selectivities and activities of the catalysts formed having the monodentate ligands is difficult because two rhodium complexes ($HRhL(CO)_3$ and $HRhL_2(CO)_2$) are present in each system and the ratio between these two complexes is not equal in the four systems. An effect of the decreasing bulkiness of the ligands on the selectivity in the hydroformylation reaction is not observed. A rhodium complex of composition $HRhL_2(CO)_2$ is more selective than a complex with the structure $HRhL(CO)_3$. All catalyst mixtures tested show approximately the same selectivity, because the amount of $HRhL_2(CO)_2$ increases with decreasing bulkiness of the ligand.

Table 11. Hydroformylation Results of 1-Octene with L = 2a−d,f and 5a−c[a]

L	L/Rh	conversn (%)	l/b	TOF[b]	linear (%)	isomerizn[c] (%)
2a	100	26	3.9	431	51	36
2b	100	29	6.8	780	83	4
2c	10	30	3.1	1600	59	22
2d	10	32	2.2	7950	64	7
2f[d]	5	26	10.4	381	86	5
5a[e]	16	21	1.2	520	48	13
5b[e]	2.5	27	2.2	1550	55	20
5c[f]	5	30	49	250	94	4

[a] Conditions: $T = 80$ °C, $p_{CO} = p_{H_2} = 10$ bar, [Rh] = 0.2 mM, [1-octene] = 0.64 M in toluene. [b] In units of (mol of aldehyde) (mol Rh)$^{-1}$ h^{-1}. [c] Formation of 2-octene. [d] [Rh] = 2 mM. [e] [Rh] = 0.4 mM, [1-octene] = 1 M.[30] [f] [Rh] = 1 mM, [1-octene] = 0.64 M.[29]

Ligands **1c**,**d** were tested under the same conditions as **1a**,**b**, although we observed decomposition of the hydride complexes of the former ligands during the spectroscopic experiments. Variation of the ligand concentrations (Rh/P = 1/50, 1/100, 1/200) showed that the best results were obtained (activity versus selectivity and isomerization) for Rh/L = 1/100. Probably, the lower rhodium and higher ligand concentrations used in the catalysis experiments compared to the spectroscopic experiments decrease the decomposition rate of the catalyst.

We were aiming at a catalyst system with improved activity compared to a catalyst system based on monodentate phosphine ligands and improved selectivity compared to catalyst systems based on monodentate phosphite ligands. The present monodentate ligands form a significant amount of $HRhL(CO)_3$, which unfortunately still gives low linear-to-branched ratios, albeit at high rates. To obtain higher selectivities, we turned to bidentate ligands.

The bidentate ligands (**2a**−**d**,**f**) are more electron withdrawing than phosphines and introduce more steric hindrance close to the rhodium center than phosphites. The spectroscopic experiments described in the previous section showed that these ligands form stable, well-defined rhodium complexes having the structure $HRhL\cap L(CO)_2$. The results obtained in the hydroformylation reaction using these bidentate ligands are presented in Table 11. Ligand **2e** was not used in the hydroformylation reaction, because no hydride complex is formed under hydroformylation conditions. The systems are less active than the catalyst systems derived from the monodentate ligands (**1a**−**d**), because the rhodium center is more electron rich when two phos-

(40) van Rooy, A.; Orij, E. N.; Kamer, P. C. J.; van Leeuwen, P. W. N. M. *Organometallics* **1995**, *14*, 34.

Chart 3

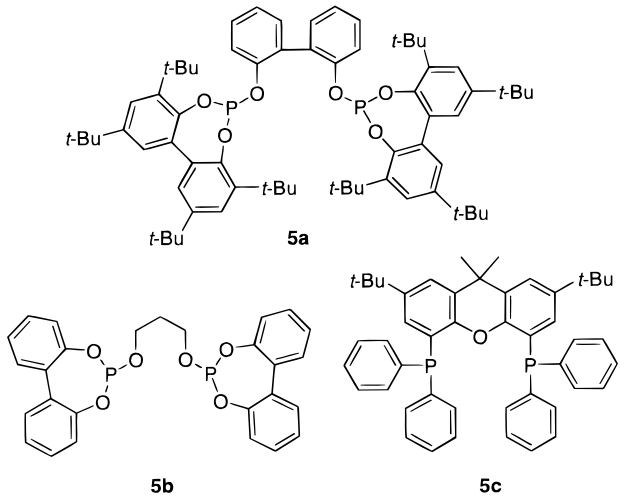

phorus ligands are attached to it. The selectivity is improved compared to that of monodentate ligand systems. The difference in activity and selectivity of the various bidentate ligands is less straightforward. The selectivities of the catalysts formed from ligands **2a**,**c** are lower than expected, in view of the phenyl substituents at the nitrogen atoms. The ratio of 2-octene is high compared to other ligands in this work. In the HP NMR and HP IR experiments we saw that complete conversion to a hydride complex is reached, although the carbonyl frequencies of the hydride complexes formed with **2a**,**c** are found at slightly higher wavenumbers than the wavenumbers observed for the hydride complexes using **2b**,**d**,**f**. This led us to conclude that the compounds assume a distorted-trigonal-bipyramidal structure. We now tentatively propose that coordination of carbon monoxide after the hydride migration is relatively slow in the distorted complexes (L∩L is a bidentate ligand), thus giving a high preference for β-hydride elimination and thus isomerization.[30]

When we compare the hydroformylation results obtained using **2b**,**d**,**f** with respect to the selectivity for the linear aldehyde, we see that both the backbone and the substituents on the phosphorus atoms determine the selectivity of the reaction. Comparison of the results of **2b**,**d** with those of phosphite ligands derived from the same backbones (**5a**,**b**; Chart 3)[31] shows that the selectivity for the linear aldehyde is improved by the introduction of the nitrogen substituents without any decrease in activity. The backbone used for ligand **2f** has proven to form very selective hydroformylation catalysts[30] for phosphorus substituents of the type PAr_2. Also for these novel phosphorus diamide ligands the xanthene backbone provided the most selective ligand, but aryl substituents on the phosphorus atom give far higher linear over branched ratios (65).

Conclusions

The introduction of nitrogen substituents on the phosphorus atom leads to very bulky π-acidic ligands, thereby combining the good properties of phosphine and phosphite ligands with respect to the hydroformylation reaction of terminal alkenes. The monodentate ligands form a significant proportion of $HRhL(CO)_3$. These complexes are very active in the hydroformylation reaction, although the linear over branched ratio is low. The bidentate ligands form catalysts with the structure $HRhL\cap L(CO)_2$, which are active and selective hydroformylation catalysts. The combination of ideal elements (backbone (and thus bite angle), steric bulk, and π-acidity) does not lead to a superior catalyst compared to catalysts containing PAr_2 and $P(OAr)_2$ substituents. It seems that the aryl substituents in PAr_2 and $P(OAr)_2$ play a very specific role in determining the shape of a *selective* catalytic site.

Experimental Section

General Information. All preparations were carried out under an atmosphere of argon using standard Schlenk techniques. Solvents were distilled from sodium/benzophenone. All glassware was dried by heating under vacuum. Column chromatography was performed using silica gel 60 (230−400 mesh) obtained from Merck or activated neutral alumina 50−200 μm obtained from Acros Organics. The NMR spectra were recorded on a Bruker AMX-300 spectrometer (^{1}H, ^{31}P, ^{13}C); the high-pressure NMR spectra were recorded on a Bruker DRX-300 spectrometer. Chemical shifts are given in ppm referenced to TMS or H_3PO_4 (external). IR spectra (high pressure) were recorded on a Nicolet 510 FT-IR spectrometer.

Hydroformylation experiments were performed in a stainless steel autoclave (196 mL). The autoclave is mechanically stirred and equipped with a reservoir, a pressure transducer, a thermocouple, and a sampling device. In a typical experiment the autoclave was flushed four times with 4 bar of syngas. $Rh(acac)(CO)_2$ and the ligand were dissolved in 15 mL of toluene, and this solution was brought into the autoclave. After it was flushed four times with 4 bar of CO/H_2 (1/1), the autoclave was put under a pressure of 15 bar. The autoclave was heated to 80 °C. After 1 h the substrate solution (2 mL of alkene, 2 mL of toluene, and 1 mL of decane) was charged into the reservoir and added to the reaction mixture by overpressure. The initial pressure of the experiment was 20 bar. The alkene was filtered over neutral alumina to remove peroxides. During the reaction several samples were taken and immediately quenched by adding an excess of $P(O\text{-}n\text{-}Bu)_3$, to form a hydroformylation-inactive rhodium species. The samples were analyzed by GC using decane as internal standard.

High-pressure NMR experiments were performed in a 10 mm o.d. sapphire NMR tube described by Elsevier et al.[41] In a typical experiment 5 mg (0.019 mmol) of $Rh(acac)(CO)_2$ and 1, 2, 5, or 10 equiv of ligand were dissolved in 1.5 mL of toluene-d_8. For ligand **2a** CD_2Cl_2 was used because of the poor solubility in toluene. The solution was brought into the argon-flushed tube. After it was closed, the tube was flushed four times with 4 bar of syngas (CO/H_2 = 1/1) and put under a pressure of 20 bar. The tube was heated in the NMR machine to 80 °C.

High-pressure IR experiments were performed in an SS 316 50 mL autoclave equipped with IRTRAN windows (ZnS, transparent up to 700 cm^{-1}, 10 mm i.d., optical path length 0.4 mm), a mechanical stirrer, a temperature controller, and a pressure device. In a typical experiment 5 mg of $Rh(acac)(CO)_2$ and 5 or 20 equiv of ligand were dissolved in 15 mL of solvent under argon. The solution was brought into the CO/H_2 (1/1) flushed autoclave and, after flushing, pressurizing, and heating of the mixture, the autoclave was placed in the infrared spectrometer. While the samples were stirred, the IR spectra were recorded. For the ligands **1b**,**d** and **2b**,**d**,**f** cyclohexane was used as solvent during these measurements. Because of the low solubility of **1a**,**c** and **2a**,**c** freshly distilled methyltetrahydrofuran was used for these ligands.

(41) Elsevier, C. J. *J. Mol. Catal.* **1994**, *92*, 285.

Triethylbiuret was synthesized by the method describe by d'Silva et al.[42] Because ethyl isocyanate is extremely toxic, special precautions were taken to prevent inhalation and contact with the skin. Triphenylbiuret and ligand **1a** were synthesized according to a literature procedure.[25] Instead of 1 equiv of triethylamine, an excess of triethylamine was used. An extra purification step (filtration over silica, eluent CH_2Cl_2) was performed to exclude the presence of traces of triethylamine hydrochloride salt in the product. All chemicals were azeotropically dried before using. All *trans*-$RhClCOL_2$ complexes were synthesized according to a literature procedure.[29]

The complex syntheses under pressure were performed in a magnetically stirred stainless steel autoclave with a volume of 6.5 mL, which was heated in an oil bath.

***N,N′,N″*-Triethylbiuret.** A 20 g (0.17 mol) amount of 1,3-diethylurea and 100 g (1.41 mol) of ethyl isocyanate were mixed together under argon. The suspension was heated to 50 °C. During heating the diethylurea dissolved in the ethyl isocyanate. The reaction mixture was stirred for 2 days at 50 °C. After this period the excess ethyl isocyanate was distilled off and carefully destroyed with alcoholic base. Traces of ethyl isocyanate were removed by adding three 100 mL portions of benzene to the reaction mixture and distilling it off. The triethylbiuret was purified by column chromatography on silica gel (eluent 1/1 petroleum ether 40−60 °C (PE 40−60)/ethyl acetate ($R_f = 0.4$)). The product was obtained as a yellow oil: yield 23 g (72%), ^{1}H NMR ($CDCl_3$): δ 1.1 (t, 6H, $^3J_{HH} = 7$ Hz, C*H*$_3$CH$_2$NH), 1.2 (t, 3H, $^3J_{HH} = 5$ Hz, C*H*$_3$CH$_2$N(CO)$_2$), 3.3 (dq, 4H, $^3J_{HH} = 5$ Hz, $^3J_{HH} = 1$ Hz CH$_3$C*H*$_2$NH), 3.7 (q, 2H, $^3J_{HH} = 7$ Hz, CH$_3$C*H*$_2$N(CO)$_2$). ^{13}C NMR ($CDCl_3$): 14.1 (s, *C*H$_3$CH$_2$N(CO)$_2$), 15.1 (s, *C*H$_3$CH$_2$NH), 35.6 (s, CH$_3$*C*H$_2$NH), 38.0 (s, CH$_3$*C*H$_2$N(CO)$_2$), 156.2 (s, N(*C*O)$_2$). IR (CH_2Cl_2) ν_{CO} 1696 (vs), 1644 (vs), ν_{NH} 1542 (vs), 1509 cm^{-1} (vs). FAB/MS: *m/e* 188. Anal. Calcd for $C_8H_{17}N_3O_2$: C, 51.32; H, 9.15. Found: C, 51.33; H, 9.39.

1,3,5-Triethylbiuret Phenylphosphorus Diamide (1b). A solution of 1.9 g (11 mmol) $PPhCl_2$ in 10 mL of toluene was added dropwise to a solution of 2.0 g (11 mmol) of *N,N′,N″*-triethylbiuret (**1**) in 40 mL of toluene and 5 mL of triethylamine (excess) at room temperature. During addition triethylamine hydrochloride precipitated. When the addition was completed, the mixture was stirred overnight at 80 °C. Another 5 mL of triethylamine was added, and the mixture was stirred another 4 h at 80 °C to complete the reaction. The mixture was cooled to room temperature, the salts were filtered off, and the toluene was evaporated under vacuum. The product was purified by column chromatography on silica gel (4/1 PE 40−60/ethyl acetate ($R_f = 0.5$)). Yield: 1.86 g (58%). Mp: 52 °C. ^{1}H NMR (C_6D_6): δ 1.0 (t, 3H, $^3J_{HH} = 7$ Hz, C*H*$_3$CH$_2$N(CO)$_2$), 1.2 (t, 6H, $^3J_{HH} = 7$ Hz, C*H*$_3$CH$_2$NP), 3.3 (dq, 2H, $^3J_{HH} = 7$ Hz, $^3J_{PH} = 7$ Hz, CH$_3$C*H*$_2$NP), 3.8 (dq, 2H, $^3J_{HH} = 7$ Hz, $^3J_{PH} = 7$ Hz, CH$_3$C*H*$_2$NP), 4.0 (q, 2H, $^3J_{HH} = 7$ Hz, CH$_3$C*H*$_2$N(CO)$_2$), 7.3−6.9 (m, 5H, *o,m,p*-PhP). ^{31}P{^{1}H} NMR (C_6D_6): δ 63.4 (s). ^{13}C NMR ($CDCl_3$) δ 13.3 (s, *C*H$_3$CH$_2$N(CO)$_2$), 15.3 (d, $^3J_{CP} = 5$ Hz, *C*H$_3$CH$_2$NP), 38.5 (s, CH$_3$*C*H$_2$N(CO)$_2$), 43.8 (d, $^2J_{CP} = 33$ Hz, CH$_3$*C*H$_2$NP), 128.9−130.3 (s, *o,m,p*-PhP), 139.8 (d, $^1J_{CP} = 24$ Hz, *ipso*-Ph), 154.7 ppm, (d, $^2J_{CP} = 7$ Hz, CO). IR (CH_2Cl_2): ν_{CO} 1692 (vs), 1658 cm^{-1} (vs). FD-MS: FD$^+$ = 293, Anal. Calcd for $C_{14}H_{20}N_3O_2P$: C, 57.33; H, 6.87; N 14.33. Found: C, 57.23; H, 6.93; N, 14.02.

1,3,5-tTriphenylbiuret Phenoxyphosphorus Diamide (1c). A solution of 1.03 g (11 mmol) of phenol in 10 mL of THF was added to a solution of 2.77 g (11 mmol) of *N,N′,N″*-triphenylbiuret phosphorus chloride in 50 mL of THF and 5 mL of triethylamine (excess) at room temperature. Triethylamine hydrochloride precipitated directly. The reaction is complete after 1 h of stirring at room temperature, and the salts are filtered off. The THF was removed under vacuum. The product was filtered over neutral alumina to remove traces of triethylamine salts (eluent CH_2Cl_2, $R_f = 1$). Yield: 3.15 g (98%) of a white powder. Mp: 169 °C. ^{1}H NMR ($CDCl_3$): δ 7.6−7.0 ppm (m, *o,m,p*-Ph). ^{31}P{^{1}H} NMR ($CDCl_3$): δ 86.3 ppm (s). ^{13}C NMR ($CDCl_3$): δ 120.6 (d, $^3J_{CP} = 6$ Hz, *o*-PhOP), 125.1 (s, *p*-PhOP), 128.5 (s, *o*-PhN(CO)$_2$), 128.6 (s, *p*-PhN(CO)$_2$), 128.6 (d, $^3J_{CP} = 7$ Hz, *p*-PhNP), 129.0 (d, $^2J_{CP} = 11$ Hz, *o*-PhNP), 129.7 (s, *m*-PhN(CO)$_2$), 130.5 (s, *m*-PhOP), 136.5 (s, *ipso*- PhN(CO)$_2$), 152.0 (d, $^2J_{CP} = 6$ Hz, CO) 152.4 (s, *ipso*-PhOP). IR (CH_2Cl_2): ν_{CO} 1717 (vs), 1681 cm^{-1} (vs). FAB/MS: *m/e* 454, Anal. Calcd for $C_{26}H_{20}N_3O_3P$: C, 68.87; H, 4.45; N, 9.27. Found: C, 68.71; H, 4.54; N, 9.11.

Crystallization of the product from absolute ethanol gave colorless crystals suitable for crystal structure determination.

1,3,5-Triethylbiuret Phenoxyphosphorus Diamide (1d). A solution of 2.3 mL (26.7 mmol) of phosphorus trichloride in 20 mL of toluene was added dropwise to a solution of 5 g (26.7 mmol) of *N,N′,N″*-triethylbiuret in 80 mL of toluene and 20 mL of triethylamine (excess) at room temperature. Triethylamine hydrochloride precipitated directly. The reaction mixture was stirred overnight at 80 °C. The mixture was cooled to room temperature, the precipitate was filtered off, and the toluene was evaporated under vacuum. The phosphorus chloride compound was obtained as a yellow oil and used directly without further purification. The purity of the compound was checked by NMR. A solution of 2.3 g (24 mmol) of phenol in 10 mL of THF was added dropwise to a solution of 6.2 g (24 mmol) of *N,N′,N″*-triethylbiuret phosphorus chloride in 50 mL of THF and 5 mL of triethylamine (excess). The reaction mixture was stirred at room temperature for 1 h. The triethylamine salts were filtered off, and the THF was evaporated. The product was filtered over alumina to remove traces of triethylamine salts (eluent CH_2Cl_2). The product was obtained as a white powder after crystallization from pentane. Yield: 5.3 g (65%). Mp: 49 °C. ^{1}H NMR ($CDCl_3$): δ 0.9 (t, 3H, $^3J_{HH} = 7$ Hz, C*H*$_3$CH$_2$N(CO)$_2$), 1.3 (t, 6H, $^3J_{HH} = 7$ Hz, C*H*$_3$CH$_2$NP), 3.6 (m, 4H, CH$_3$C*H*$_2$NP and CH$_3$C*H*$_2$N(CO)$_2$), 3.9 (m, 2H, CH$_3$C*H*$_2$NP), 6.8 (d, 2H, $^3J_{HH} = 8$ Hz, *o*-PhOP), 7.1 (t, 1 H, $^3J_{HH} = 7$ Hz, *p*-PhOP), 7.3 (t, 2 H, $^3J_{HH} = 8$ Hz, *m*-PhOP). ^{31}P{^{1}H} NMR ($CDCl_3$): δ 87.4 (s). ^{13}C NMR ($CDCl_3$): δ 13.3 (s, *C*H$_3$CH$_2$N(CO)$_2$), 15.3 (s, *C*H$_3$CH$_2$NP), 38.5 (s, CH$_3$*C*H$_2$N(CO)$_2$), 42.6 (d, $^2J_{CP} = 35$ Hz, CH$_3$*C*H$_2$NP), 121.0 (d, $^3J_{CP} = 35$ Hz, *o*-PhOP), 125.0 (s, *p*-PhOP), 130.0 (s, *m*-PhOP), 151.0 (d, $^2J_{CP} = 6$ Hz, *ipso*-PhOP), 152.1 (d, $^2J_{CP} = 9$ Hz, CO). IR (CH_2Cl_2): ν_{CO} 1699 (vs), 1656 cm^{-1} (vs). FAB/MS: *m/e* 310. Anal. Calcd for $C_{14}H_{20}N_3O_3P$: C, 54.37; H, 6.52; N 13.59. Found: C, 54.60; H, 6.61; N, 13.47.

Compound 2a. A 2.2 g (12 mmol) amount of 2,2′-hydroxy-1,1′-biphenyl dissolved in 20 mL of toluene was added dropwise to a solution of 2.4 g (6 mmol) of *N,N′,N″*-triphenylbiuret phosphorus chloride and 7.6 mL (60 mmol) of triethylamine in 100 mL of toluene at room temperature. When the addition was completed, the mixture was stirred at 80 °C for 4 h. The triethylamine salts were filtered, and the solvent was removed under vacuum. Purification by column chromatography on silica gel (eluent 7/3 PE (60−80)/EtOAc, $R_f = 0.15$) gave a white solid, Yield: 5.2 g (95%). Mp: 284 °C dec. ^{1}H NMR ($CDCl_3$): δ 6.9−7.4 (m, *o,m,p*-Ph). ^{31}P{^{1}H} NMR ($CDCl_3$): δ 91.0 (s). ^{13}C NMR ($CDCl_3$): δ 129.1, 128.7, 127.8 (s, *o,m,p*-Ph−N), 129.3 (s, *ipso*-Ph−O−P), 132.4−118.1 (s, *o,m,p*-Ph−O), 136.2 (s, *ipso*-Ph−N−P), 137.3 (s, *ipso*-Ph−N−P), 137.5 (s, *ipso*-Ph−N−P), 149.9 (s, CO), 151.6 (d, $^2J_{CP} = 4$ Hz, CO). IR (CH_2Cl_2): ν_{CO} 1719 (vs), 1685 (vs). FAB/MS: *m/e* 905. Anal. Calcd for $C_{52}H_{38}N_6O_6P_2$: C, 69.03; H, 4.20; N 9.29. Found: C, 68.84; H, 4.36; N, 9.08.

Crystallization of the product from absolute ethanol gave colorless crystals suitable for crystal structure determination.

Compound 2b. A solution of 2.0 mL (23 mmol) of phosphorus trichloride in 20 mL of toluene was added dropwise to a solution of 4.2 g (23 mmol) of *N,N′,N″*-triethylbiuret in 80

(42) d'Silva, T. D. J.; Lopes, A.; Jones, R. L.; Singhawangcha, S.; Chan, J. K. *J. Org. Chem.* **1986**, *51*, 3781.

mL of toluene and 20 mL of triethylamine (excess) at room temperature. Triethylamine hydrochloride precipitated directly. The reaction mixture was stirred overnight at 80 °C. The mixture was cooled to room temperature, the precipitate was filtered off, and the toluene was evaporated under vacuum. The phosphorus chloride compound was obtained as a yellow oil and used directly without further purification. The purity of the compound was checked by NMR. A solution of 2.1 g (11 mmol) of 2,2′-hydroxy-1,1′-biphenyl in 10 mL of THF was added dropwise to a solution of 5.6 g (22 mmol) of *N,N′,N″*-triethylbiuret phosphorus chloride in 50 mL of THF and 10 mL of triethylamine (excess). The reaction mixture was stirred at room temperature for 1 h. The triethylamine salts were filtered off, and the THF was evaporated. The product was purified by filtration over neutral alumina to remove phosphite impurities with toluene as eluent. The product is flushed from the column with 1/1 PE (40−60)/EtOAc. The product was obtained as a colorless oil that crystallized after 1 week. Yield: 4.9 g (73%). Mp: 76 °C. ^{1}H NMR ($CDCl_3$): δ 0.9 (t, 6H, $^3J_{HH}$ = 7 Hz, CH_3CH$_2$N(CO)$_2$), 1.1 (t, 12H, $^3J_{HH}$ = 7 Hz, CH_3-CH$_2$NP), 2.9 (m, 4H, CH$_3$CH_2N(CO)$_2$), 3.5 (q, 8H, $^3J_{HH}$ = 7 Hz, CH$_3$CH_2NP), 6.9 (d, 2H, $^3J_{HH}$ = 8 Hz, *o*-Ph), 7.2 (m, 6H, *m,p*-Ph). ^{31}P{^{1}H} NMR ($CDCl_3$): δ 89.9 (s). ^{13}C NMR ($CDCl_3$): δ 13.4 (s, *C*H$_3$CH$_2$N(CO)$_2$), 15.1 (s, *C*H$_3$CH$_2$NP), 39.4 (s, CH$_3$CH_2N-(CO)$_2$), 41.9 (d, $^2J_{CP}$ = 35 Hz, CH$_3$CH$_2$NP), 120.8−132.5 (*m,p*-Ph), 130.5 (s, *o*-Ph), 149.2 (d,$^2J_{CP}$ = 3 Hz, *ipso*-Ph), 151.9 (d, $^2J_{CP}$ = 8 Hz, CO). IR (CH_2Cl_2): ν_{CO} 1702 (vs), 1660 cm^{-1} (vs). FAB/MS: *m/e* 617. Anal. Calcd for $C_{28}H_{38}N_6O_6P_2$: C, 54.54; H, 6.21; N, 13.63. Found: C, 54.80; H, 6.23; N, 13.31.

Compound 2c. A 0.5 g (4.6 mmol) amount of 2,2′-dimethyl-1,3-propanediol dissolved in 10 mL of THF was added dropwise to a solution of 3.6 g (9.2 mmol) of *N,N′,N″*-triphenylbiuret phosphorus chloride and 10 mL (excess) of triethylamine in 150 mL of toluene at room temperature. When the addition was completed, the mixture was stirred for 1 h at room temperature. The triethylamine salts were filtered, and the solvent was concentrated to 20 mL. The product was filtered and washed with 60 mL of diethyl ether. The product was dissolved in dichloromethane, and this solution was washed with water. After evaporation of the dichloromethane the white solid was washed with 20 mL of ether. Yield:1.6 g (43%). Mp: 240−242 °C dec. ^{1}H NMR ($CDCl_3$): δ 1.1 (s, CH_3, 6H), 3.9 (d,$^3J_{PH}$ = 5 Hz, CH_2, 4H), 7.4−7.2 (m, Ph, 30H). ^{31}P{^{1}H} NMR ($CDCl_3$): δ 83.1 (s). ^{13}C NMR ($CDCl_3$): δ 21.8 (s, *C*(*C*H$_3$)$_2$), 36.5 (s, *C*H$_2$), 69.6 (s, *C*(CH$_3$)$_2$), 129.3−128.1 (m, *o,m,p*-Ph−N), 137.2 (s, *ipso*-Ph-(N(CO)$_2$), 137.6 (d, $^2J_{PC}$ = Hz, *ipso*-Ph−N−P), 152.3 (*C*O(NPh)$_2$), 152.4 (s, *C*O−N−P). IR (CH_2Cl_2): ν_{CO} 1714 (vs), 1673 cm^{-1} (vs). FAB/MS: *m/e* 823. Anal. Calcd for $C_{45}H_{40}$-$N_6O_6P_2$: C, 65.69; H, 4.87; N, 10.22. Found: C, 65.17; H, 4.94; N, 10.16.

Compound 2d. A solution of 2.3 mL (26 mmol) of phosphorus trichloride in 20 mL of toluene was added dropwise to a solution of 4.9 g (26 mmol) of *N,N′,N″*-triethylbiuret in 80 mL of toluene and 20 mL of triethylamine (excess) at room temperature. Triethylamine hydrochloride precipitated directly. The reaction mixture was stirred overnight at 80 °C. The mixture was cooled to room temperature, the precipitate was filtered off, and the toluene was evaporated under vacuum. The phosphorus chloride compound was obtained as a yellow oil and used directly without further purification. The purity of the compound was checked by NMR. A solution of 1.1 g (10 mmol) of 2,2′-dimethyl-1,3-propanediol in 10 mL of THF was added dropwise to a solution of 5.13 g (20 mmol) of *N,N′,N″*-triethylbiuret phosphorus chloride in 50 mL of THF and 10 mL of triethylamine (excess). The reaction mixture was stirred at room temperature for 1 h. The triethylamine salts were filtered off, and the THF was evaporated. The product was purified by column chromatography over neutral alumina (eluent 4/1 PE (40−60)/EtOAc, R_f = 0.6). The product was obtained as a white powder. Yield: 3.2 g (60%). Mp: 56 °C. ^{1}H NMR ($CDCl_3$): δ 0.8 (s, 6H, Me) 1.1 (t, 6H, $^3J_{HH}$ = 7 Hz, CH_3CH$_2$N(CO)$_2$), 1.3 (t, 12H, $^3J_{HH}$ = 7 Hz, CH_3CH$_2$NP), 3.2 (d, 4H, $^3J_{HP}$ = 5 Hz, CH_2OP), 3.5 (m, 8H, CH$_3$CH_2NP), 3.9 (q, 4H, $^3J_{HH}$ = 7 Hz, CH$_3$CH_2N(CO)$_2$). ^{31}P{^{1}H} NMR ($CDCl_3$): δ 85.4 (s). ^{13}C NMR ($CDCl_3$): δ 13.7 (s, *C*H$_3$CH$_2$N(CO)$_2$), 16.1 (s, *C*H$_3$CH$_2$NP), 21.6 (s, *C*(*C*H$_3$)$_2$), 36.2 (d, $^2J_{CP}$ = 3 Hz, *C*H$_2$-OP), 38.2 (s, CH$_3$CH$_2$N(CO)$_2$), 42.4 (d, $^2J_{CP}$ = 35 Hz, CH$_3$*C*H$_2$-NP), 68.5 (d, $^3J_{CP}$ = 6 Hz, *C*(CH$_3$)$_2$), 152.7 (d, $^2J_{CP}$ = 10 Hz, *C*O),. IR (CH_2Cl_2): ν_{CO} 1695 (vs), 1653 cm^{-1} (vs). FD-MS: FD$^+$ = 534. Anal. Calcd for $C_{21}H_{40}N_6O_6P_2$: C, 47.19; H, 7.54; N, 15.72. Found: C, 47.07; H, 7.43; N, 15.47.

Compound 2e. A 3.2 mL (7.3 mmol) amount of *n*-BuLi (2.5 M in hexane) was added dropwise to a solution of 1.69 g (3.6 mmol) of 4,5-dibromo-2,7-di-*tert*-butyl-9,9-dimethylxanthene in 70 mL of THF at −60 °C. The suspension was stirred for 1 h at −60 °C. The reaction mixture was slowly warmed to 0 °C. A 2.89 g (7.3 mmol) amount of *N,N′,N″*-triphenylbiuret phosphorus chloride in 10 mL of THF was added dropwise to the suspension at −60 °C. The reaction mixture was slowly warmed to room temperature. The solution was filtered over neutral alumina, and the THF was evaporated. The white solid was crystallized from acetonitrile/methanol. Yield: 2.8 g (76%). Mp: 341 °C. ^{1}H NMR (acetone-d_6): δ 1.5 (s, 18H, *t*-Bu), 1.9 (s, 6H, (C*H*$_3$)$_2$C), 6.8, 7.0, 7.4 (m, 30H, *o,m,p*-PhN), 7.6 (m, (broad), 2H, C*H*CC(CH$_3$)$_2$CC*H*), 8.0 (d, $^3J_{PH}$ = 2 Hz, C*H*CP). ^{31}P{^{1}H} NMR ($CDCl_3$): δ 69.6 (s). ^{13}C NMR ($CDCl_3$): δ 31.8 (s, (*C*H$_3$)$_3$C), 33.4 (s, (*C*H$_3$)$_2$C), 34.9 (s, (CH$_3$)$_2$*C*), 35.2 (s, (CH$_3$)$_3$*C*), 124.4−129.2 (aromatic C xanthene backbone and *o,m,p*-NPh), 130.5 (s, *m*-PhC(CH$_3$)$_2$), 137.0 (s, *m*-PhC(CH$_3$)$_3$), 140.1 (t, *o*-OPhP), 154.3 (s, CO). IR (CH_2Cl_2): ν_{CO} 1706 (vs), 1675 (vs), 1670 cm^{-1} (sh). FAB/MS: *m/e* 1041.3. Anal. Calcd for $C_{63}H_{58}N_6O_5P_2$: C, 72.68; H, 5.62; N, 8.07. Found: C, 72.17; H, 5.72; N, 8.03.

Compound 2f. A solution of 1.37 g of (10 mmol) of phosphorus trichloride in 20 mL of toluene was added dropwise to a solution of 1.9 g (10 mmol) of *N,N′,N″*-triethylbiuret in 80 mL of toluene and 10 mL of triethylamine (excess) at room temperature. Triethylamine hydrochloride precipitated directly. The reaction mixture was stirred overnight at 80 °C. The mixture was cooled to room temperature, the precipitate was filtered off, and the toluene was evaporated under vacuum. The phosphorus chloride compound was obtained as a yellow oil and used directly without further purification. The purity of the compound was checked by NMR. A 3.96 mL (9.9 mmol) amount of *n*-BuLi (2.5 M in hexane) was added dropwise to a solution of 2.11 g (4.5 mmol) of 4,5-dibromo-2,7-di-*tert*-butyl-9,9-dimethylxanthene in 70 mL of THF at −60 °C. The suspension was stirred for 1 h at −60 °C. The reaction mixture was slowly warmed to 0 °C. A 2.27 g (9 mmol) amount of *N,N′,N″*-triethylbiuret phosphorus chloride in 10 mL of THF was added dropwise to the suspension at −60 °C. The reaction mixture was slowly warmed to room temperature. The solution was filtered over neutral alumina, and the THF was evaporated. The white solid was washed with hot methanol. Yield: 3.1 g (92%). Mp: 259 °C. ^{1}H NMR ($CDCl_3$): δ 1.2 (m, 18H, C*H*$_3$CH$_2$N), 1.3 (s, 18H, *t*-Bu), 1.6 (s, 6H, (C*H*$_3$)$_2$C), 3.8 (m, 12H, CH$_3$C*H*$_2$N), 7.0 (s (broad), 2H, C*H*CC(CH$_3$)$_2$CC*H*), 7.4 (d, $^3J_{PH}$ = 2 Hz, C*H*CP). ^{31}P{^{1}H} NMR ($CDCl_3$): δ 57.1 (s). ^{13}C NMR ($CDCl_3$): δ 13.6 (s, *C*H$_3$CH$_2$N(CO)), 14.7 (s, *C*H$_3$CH$_2$NP), 31.1 (s, (*C*H$_3$)$_3$C), 33.0 (s, (*C*H$_3$)$_2$C), 34.5 (s, (CH$_3$)$_2$*C*), 39.2 (s, CH$_3$*C*H$_2$N(CO)), 43.0 (d, $^2J_{CP}$ = 21 Hz, CH$_3$*C*H$_2$NP), 43.4 (s, (CH$_3$)$_3$*C*), 123.9 (d, J_{CP} = 39 Hz, *ipso*-PPh), 124.6 (s, *p*-PhP), 126.5 (s, *o*-PhP), 129.6 (s, *m*-PhC(CH$_3$)$_2$), 145.8 (s, *m*-PhC-(CH$_3$)$_3$), 150.0 (t, *o*-OPhP), 154.5 (d, $^2J_{CP}$ = 4 Hz, CO). IR (CH_2-Cl_2): ν_{CO} 1688 (vs), 1653 cm^{-1} (vs). FAB/MS: *m/e* 754. Anal. Calcd for $C_{39}H_{58}N_6O_5P_2$: C, 62.22; H, 7.77; N, 11.16. Found: C, 62.06; H, 7.75; N, 11.02.

***trans*-RhClCO(1a)$_2$ (3a).** A solution of 176 mg (0.4 mmol) of **1a** in 2 mL of CH_2Cl_2 was added dropwise to a solution of 39 mg (0.1 mmol) of [Rh(CO)$_2$Cl]$_2$ in 2 mL of CH_2Cl_2. When the ligand was added, CO evolved from the solution directly. The yellow solution was stirred for 1 h at room temperature.

After 1 h the solvent was concentrated to 1 mL and 10 mL of pentane was added. The complex precipitated directly. The complex was filtered off and washed with hot benzene. This resulted in a pure yellow powder. Yield: 177 mg (85%). Mp: 239 °C dec. ^{1}H NMR ($CDCl_3$): δ 7.7−7.1 (m, aromatic H). ^{31}P{^{1}H} NMR ($CDCl_3$): δ 101.2 (doublet, $^1J_{RhP}$ = 166 Hz). ^{13}C NMR (CD_2Cl_2): δ 130.5−135.3 (*o,m,p*-Ph), 138.9−139.3 (*ipso*-Ph), 154.1 (N*C*O); the signal of the carbonyl ligand was not obtained in ^{13}C NMR because of the combination of low intensity of the signal and low solubility of the compound. IR (CH_2Cl_2): ν_{CO} 1719 (vs), 1694 (vs), 1676 cm^{-1}, ν_{Rh-CO} 2004 cm^{-1} (vs). FAB/MS: *m/e* [RhClCO(**1a**)$_2$]$^+$ 1041, [RhCO(**1a**)$_2$]$^+$ 1005, [Rh(**1a**)$_2$]$^+$ 976. Anal. Calcd for $C_{53}H_{40}N_6O_5P_2ClRh\cdot CH_2Cl_2$: C, 60.16; H, 3.93; N, 7.79. Found: C, 60.19; H, 4.02; N, 7.97.

***trans*-RhClCO(1b)$_2$ (3b).** A solution of 117 mg (0.4 mmol) of **1b** in 2 mL of CH_2Cl_2 was added dropwise to a solution of 39 mg (0.1 mmol) of [Rh(CO)$_2$Cl]$_2$ in 2 mL of CH_2Cl_2. When the ligand was added, CO evolved from the solution directly. The yellow solution was stirred for 1 h at room temperature. After 1 h the solvent was concentrated to 1 mL and 10 mL of pentane was added. The complex precipitated directly. The complex was filtered off and washed with 5 mL of pentane. This resulted in a pure yellow powder. Yield: 119 mg (79%). Mp: 158 °C dec. ^{1}H NMR (CD_2Cl_2): δ 0.7 (t, 6 H, $^3J_{HH}$ = 7 Hz, (CO)$_2$NCH$_2$C*H*$_3$), 1.3 (t, 12H, $^3J_{HH}$ = 7 Hz, PNCH$_2$C*H*$_3$), 3.6 (q, 4 H, $^3J_{HH}$ = 7 Hz, (CO)$_2$NC*H*$_2$CH$_3$), 4.0 (multiplet, PNC*H*$_2$CH$_3$), 7.4 (multiplet, *o,m,p*-PhP). ^{31}P{^{1}H} NMR (CD_6Cl_6): δ 91.1 (d, $^1J_{RhP}$ = 156 Hz). ^{13}C NMR ($CDCl_3$): δ 13.4 (s, *C*H$_3$CH$_2$NCO), 14.6 (s, *C*H$_3$CH$_2$NP), 39.4 (s, CH$_3$*C*H$_2$NCO), 44.8 (dd, J_{CP} = 10 Hz, J_{CRh} = 10 Hz, CH$_3$*C*H$_2$NP), 121.7−131.1 (*o,m,p*-PhP), 150.7 (dd, J_{CP} = 8 Hz, J_{CRh} = 8 Hz, N*C*O), 150.8 (s, *ipso*-PhP), 183.1 (dt, J_{CP} = 17 Hz, J_{CRh} = 72 Hz, Rh*C*O). IR (CH_2Cl_2): ν_{CO} 1705 (vs), 1670 cm^{-1} (vs), ν_{Rh-CO} 2010 cm^{-1}. FAB/MS: *m/e* [RhClCO(**1b**)$_2$]$^+$ 753, [RhCl(**1b**)$_2$]$^+$ 724, [RhCO(**1b**)$_2$]$^+$ 717. Anal. Calcd for $C_{29}H_{40}N_6O_5P_2ClRh$: C, 46.26; H, 5.35; N, 11.16. Found: C, 46.24; H, 5.53; N, 11.02.

***trans*-RhClCO(1c)$_2$ (3c).** A solution of 181 mg (0.4 mmol) of **1c** in 2 mL of CH_2Cl_2 was added dropwise to a solution of 39 mg (0.1 mmol) of [Rh(CO)$_2$Cl]$_2$ in 2 mL of CH_2Cl_2. When the ligand was added, CO evolved from the solution directly. The yellow solution was stirred for 1 h at room temperature. After 1 h the solvent was concentrated to 1 mL and 10 mL of pentane was added. The complex precipitated directly. The complex was filtered off and washed with hot benzene. This resulted in a pure pale yellow powder. Yield: 202 mg (94%). Mp: 161 °C dec. ^{1}H NMR ($CDCl_3$): 7.55−6.55 (m, *o,m,p*-PhN, *o,m,p*-PhOP). ^{31}P{^{1}H} NMR ($CDCl_3$): δ 105 (doublet, $^1J_{RhP}$ = 212 Hz). ^{13}C NMR (CD_2Cl_2): δ 130−129 (m, *o,p*-PhN(CO)$_2$, *o,p*-PhOP), 131.0 (s, *m*- PhN(CO)$_2$), 131.9 (s, *m*-PhOP), 135.8 (dd, *ipso*-PhOP, J_{RhC} = 4 Hz, J_{PC} = 4 Hz), 137.3 (s, *ipso*-PhN), 151.0 (s, N(*C*O)$_2$), 181.8 (dt, J_{RhC} = 73 Hz, J_{PC} = 20 Hz). IR (CH_2Cl_2): ν_{CO} 1725 (vs), 1692 cm^{-1} (vs), ν_{Rh-CO} 2021 cm^{-1} (vs). FAB/MS: *m/e* [RhClCO(**1c**)$_2$]$^+$ 1073, [RhCl(**1c**)$_2$]$^+$ 1044, [RhCO(**1c**)$_2$]$^+$ 1037**,** [Rh (**1c**)$_2$]$^+$ 1008. Anal. Calcd for $C_{53}H_{40}N_6O_7P_2ClRh$: C, 59.31; H, 3.76; N, 8.07. Found: C, 59.18; H, 3.93; N, 7.74.

Crystallization of a small fraction from CH_2Cl_2/Et_2O resulted in crystals suitable for crystal structure determination.

***trans*-RhClCO(1d)$_2$ (3d).** A solution of 124 mg (0.4 mmol) of **1d** in 2 mL of CH_2Cl_2 was added dropwise to a solution of 39 mg (0.1 mmol) of [Rh(CO)$_2$Cl]$_2$ in 2 mL of CH_2Cl_2 When the ligand was added, CO evolved from the solution directly. The yellow solution was stirred for 1 h at room temperature. After 1 h the solvent was concentrated to 1 mL and 10 mL of pentane was added. The complex precipitated directly. The yellow complex was filtered off and washed with 5 mL of pentane. Yield: 140 mg (89%). Mp: 158 °C dec. ^{1}H NMR (CD_2Cl_2): δ 0.6 (t, 6 H, $^3J_{HH}$ = 7 Hz, (CO)$_2$NCH$_2$C*H*$_3$), 1.2 (t, 12H, $^3J_{HH}$ = 7 Hz, PNCH$_2$C*H*$_3$), 3.4 (q, 4 H, $^3J_{HH}$ = 7 Hz, (CO)$_2$NC*H*$_2$CH$_3$), 4.1 (multiplet, PNC*H*$_2$CH$_3$), 6.9 (d, 4H, $^3J_{HH}$ = 8 Hz, *o*-PhOP), 7.2 (t, 2H, $^3J_{HH}$ = 7 Hz, *p*-PhOP), 7.3 (multiplet, *m*-PhOP). ^{31}P{^{1}H} NMR ($CDCl_3$) δ 101.2 (doublet, $^1J_{RhP}$ = 209 Hz), ^{13}C NMR (CD_2Cl_2): δ 15.0 (s, *C*H$_3$CH$_2$N(CO)$_2$), 16.3 (s, *C*H$_3$CH$_2$NP), 40.7 (s, CH$_3$*C*H$_2$N(CO)$_2$), 47.5 (dd, CH$_3$*C*H$_2$NP, J_{RhC} = 16 Hz, J_{PC} = 16 Hz), 130.8 (m, *o,m,p*-PhOP), 139.0 (dt, *ipso*-PhOP, J_{RhC} = 26 Hz, J_{PC} = 4 Hz), 154 (s, N(*C*O)$_2$), 185 (dt, Rh*C*O, J_{RhC} = 72 Hz, J_{PC} = 18 Hz). IR (CH_2Cl_2): ν_{CO} 1711 (vs), 1671 cm^{-1} (vs), ν_{Rh-CO} 2025 cm^{-1}. FAB/MS: *m/e* [RhClCO(**1d**)$_2$]$^+$ 785, [RhCl(**1d**)$_2$]$^+$ 756, [RhCO(**1d**)$_2$]$^+$ 749, [Rh(**1d**)$_2$]$^+$ 721. Anal. Calcd for $C_{29}H_{40}N_6O_7P_2ClRh$: C, 44.37; H, 5.14; N, 10.71. Found: C, 44.26; H, 4.91; N, 10.73.

Crystallization of a small fraction from benzene resulted in crystals suitable for crystal structure determination.

HRh(1b)$_3$CO (4). A 50 mg (0.2 mmol) amount of Rh(acac)(CO)$_2$ and 285 mg (1.0 mmol) of **1b** were dissolved in 20 mL of toluene. The solution was brought into the autoclave and pressurized to 20 bar of CO/H_2 (1/1). The autoclave was heated for 1 h at 80 °C and then heated to room temperature. After depressurization the clear red solution was brought into a Schlenk apparatus and saturated with argon. Upon standing for one night under an argon atmosphere, compound **4** was formed. Evaporation of the toluene and washing with benzene gave the pure compound **4**. Yield: 20 mg (10%). Mp: 106 °C dec. ^{1}H NMR (CD_2Cl_2): δ −10.7 (broad, hydride), 0.5 (broad, 9H, C*H*$_3$CH$_2$N(CO)$_2$), 2.1 (broad, 18H, C*H*$_3$CH$_2$NP), 3.5 (broad, 18H, CH$_3$C*H*$_2$N), 7.1 and 7.3 (broad, 15H, *o,m,p*-PhP). ^{31}P{^{1}H} NMR (CD_2Cl_2): δ 117.2 (broad doublet, $^1J_{RhP}$ = 169 Hz),; because of fluxional behavior an accurate ^{13}C NMR could not be obtained). IR (CH_2Cl_2): ν_{CO} 1695 (vs), 1660 cm^{-1} (vs), ν_{Rh-CO} 2019 cm^{-1}. FD MS: FD$^+$ 1012. Anal. Calcd for $C_{43}H_{61}N_9O_7P_3Rh$: C, 51.04; H, 6.08; N, 12.46. Found: C, 51.16; H, 5.91; N, 12.62.

Crystallization of a small fraction from benzene resulted in crystals suitable for crystal structure determination.

Crystal Structure Determination of 1c, 2a, and 3c,d. Detailed crystallographic information on the structures of **1c**, **2a**, and **3c**,**d** is summarized in Table 12. An Enraf-Nonius CAD-4 diffractometer with graphite-monochromated Cu Kα radiation and $\omega-2\theta$ scan was used for data collection. The intensities of two reflections were measured hourly. Unit-cell parameters were refined by a least-squares fitting procedure using 23 reflections with $80 \le 2\theta \le 84°$ (**1c**), $80 \le 2\theta \le 82°$ (**2a**, **3c**,**d**). Absorption correction was performed with the program PLATON,[43] following the method of North et al.[44] using ψ-scans of five reflections, with transmissions in the range of 0.851−0.922 (**1c**), 0.677−0.913 (**2a**), 0.497−0.989 (**3c**), and 0.589−0.991 (**3d**). The structure was solved by the PATTY option of the DIRDIF96 program system.[45] The hydrogen atom positions were calculated. After isotropic refinement of the initial model for **3c**, ΔF synthesis revealed three independent peaks, which formed a six-membered ring that was interpreted as benzene, one of the solvents used during crystallization. Full-matrix least-squares refinement on F, anisotropic for the non-hydrogen atoms and isotropic for the hydrogen atoms, the latter restrained in such a way that the carrier remained constant at approximately 1.0 Å, converged to the following: $R = 0.058$, $R_w = 0.058$ $(\Delta/\sigma)_{max} = 0.05$, $S = 0.99$ (**1c**); $R = 0.066$, $R_w = 0.070$ $(\Delta/\sigma)_{max} = 0.32$, $S = 1.063$ (**2a**); $R = 0.045$, $R_w = 0.043$ $(\Delta/\sigma)_{max} = 0.66$, $S = 1.008$ (**3c**); $R = 0.045$, $R_w = 0.049$ $(\Delta/\sigma)_{max} = 0.08$, $S = 1.094$ (**3d**). A weighting scheme of $w = [1.5 + 0.01(\sigma(F_o))^2 + 0.01/(\sigma(F_o))]^{-1}$ was used for **1c** and **2a**. A weighting scheme of $w = [7.5 + 0.01(\sigma(F_o))^2 + 0.01/(\sigma(F_o))]^{-1}$ was used for **3c**. A weighting scheme of $w = [2.5 + 0.01(\sigma(F_o))^2 + 0.01/(\sigma(F_o))]^{-1}$ was used for **3d**. The secondary isotropic extinction coefficient[46,47] was refined to Ext = 0.059(5) (**1c**),

(43) Spek, A. L. *Acta Crystallogr.* **1990**, *A46*, C34.
(44) North, A. C. T.; Phillips, D. C.; Mathews, F. S. *Acta Crystallogr.* **1968**, *A26*, 351.
(45) Beurskens, P. T.; Beurskens, G.; Bosman, W. P.; de Gelder, R.; Garcia-Granda, S.; Gould, R. O.; Israel, R.; Smits, J. M. M. The DIRDIF-96 Program System; Crystallography Laboratory, University of Nijmegen, Nijmegen, The Netherlands, 1996.

Table 12. Crystal Data and Details of the Structure Determination of 1d, 3c,d, and 2a

	1d	2a	3c	3d
empirical formula	$C_{26}H_{20}N_3O_3P$	$C_{52}H_{38}N_6O_6P_2$	$C_{29}H_{40}N_6O_7P_2ClRh\cdot C_6H_6$	$C_{53}H_{40}N_6O_7P_2ClRh$
fw	453.4	904.8	785.0	1073.2
temp, K	room temp	room temp	253 K	233
wavelength (λ, Å)			Cu Kα (1.5418)	
abs coeff, μ, cm^{-1}	13.2	13.5	51.3	44.6
cryst syst	monoclinic	triclinic	monoclinic	triclinic
space group	$P2_1/n$	$P\bar{1}$	$C2/c$	$P\bar{1}$
unit cell dimens				
a, Å	12.4340(10)	10.2617(7)	18.800(4)	10.4140(9)
b, Å	13.9618(9)	14.1002(9)	14.402(1)	11.0175(5)
c, Å	13.5501(7)	17.043(2)	15.312(3)	23.401(2)
α, deg	90	92.463(5)	90	83.941(7)
β, deg	100.467(5)	99.118(6)	98.45(1)	79.183(14)
γ, deg	90	100.740(5)	90	67.480(4)
V, Å^3	2313.2(3)	2263.9(4)	4100.8(12)	2434.4(3)
Z	4	2	2	4
density, g cm^{-3}	1.302	1.327	1.398	1.464
F(000)	944	940	1784	1096
cryst size, mm	0.25 × 0.25 × 0.55	0.25 × 0.50 × 0.50	0.30 × 0.40 × 0.65	0.30 × 0.50 × 0.60
range of data collecn, deg	$4.4 \le \theta \le 74.8$	$2.6 \le \theta \le 74.8$	$3.9 \le \theta \le 74.7$	$3.8 \le \theta \le 74.8$
index range	$0 \le h \le 15$	$-12 \le h \le 12$	$-23 \le h \le 0$	$-13 \le h \le 0$
	$0 \le k \le 17$	$-17 \le k \le 17$	$0 \le k \le 17$	$-13 \le k \le 12$
	$-16 \le l \le 16$	$0 \le l \le 21$	$-18 \le l \le 19$	$-29 \le l \le 28$
no. of rflns collcd	4755	9294	4205	10 043
final R	0.058 (for 3799 obsd rflns)	0.066 (for 7167 obsd rflns)	0.045 (for 3874 obsd rflns)	0.045 (for 9660 obsd rflns)

0.207(8) (**2a**), 0.116(4) (**3c**), 0.291(7) (**3d**). A final difference Fourier map revealed a residual electron density between −0.38 and 0.67 e Å^{-3} (**1c**), −0.45 and 0.42 e Å^{-3} (**2a**), −0.9 and 1.19 e Å^{-3} (**3c**), and −2.0 and 1.44 e Å^{-3} (**3d**) in vicinity of the heavy atoms. Scattering factors were taken from refs 48 and 49. The anomalous scattering of Rh, Cl, and P was taken from ref 48. All calculations were performed with XTAL,[50] unless stated otherwise.

Crystal Structure Determination of 4. Crystal data: $C_{43}H_{61}N_9O_7P_3\cdot 3C_6H_6$, fw = 1246.15, yellow block, 0.55 × 0.30 × 0.10 mm^3, trigonal, $R3c$ (No. 161), $a = b = 23.2546(17)$ Å, $c = 19.624(2)$ Å, $\gamma = 120°$, $V = 9190.4(13)$ Å^3, $Z = 6$, $\rho = 1.351$ g cm^{-3}. Intensities were measured on an Enraf-Nonius CAD4T diffractometer with a rotating anode (Mo Kα, $\lambda = 0.710\ 73$ Å) at a temperature of 150 K. Absorption correction was based on ψ-scans (PLATON,[51] $\mu = 0.416$ mm^{-1}, 0.86−0.97 transmission): 18 616 measured reflections, 4700 unique reflections ($R_{int} = 0.0773$). The structures were solved with direct methods (SIR-97)[52] and refined with the program SHELXL-97[53] as an inversion twin against F^2 of all reflections up to a resolution of $((\sin\theta)/\lambda)_{max} = 0.65$ Å^{-1}. The Flack x parameter was determined as 0.54(4). Non-hydrogen atoms were refined freely with anisotropic displacement parameters. The hydride hydrogen atom was fixed in a calculated position; the other hydrogen atoms were refined as rigid groups. The drawings, calculations, and checking for higher symmetry were performed with the PLATON package.[51] $R(I > 2\sigma(I))$: R1 = 0.0452, wR2 = 0.1016. R(all data): R1 = 0.0591, wR2 = 0.1078. $S = 1.046$.

Acknowledgment. The crystal structure determination of complex **4** was in part supported (M.L., A.L.S.) by the Council for Chemical Sciences of The Netherlands Organization for Scientific Research (CW-NWO).

Supporting Information Available: Listings of crystal data and collection parameters, atomic coordinates, bond lengths, bond angles, and thermal displacement parameters for compounds **1c**, **2a**, **3c**,**d**, and **4**. This material is available free of charge via the Internet at http://pubs.acs.org.

OM9910120

(46) Zachariasen, W. H. *Acta Crystallogr.* **1967**, *A23*, 558.
(47) Larson, A. C. *Crystallogr. Comput.* **1969**, 291.
(48) Cromer, D. T.; Mann, J. B. *Acta Crystallogr.* **1968**, *A24*, 321.
(49) *International Tables for X-ray Crystallography*; Kynoch Press: Birmingham, U.K., 1974; Vol. IV, p 55.
(50) Hall, S. R., King, G. S. D., Stewart, J. M., Eds. *XTAL3.4 User's Manual*; University of Western Australia, Lamb, Perth, Australia, 1995.
(51) Spek, A. L. PLATON, A Multipurpose Crystallographic Tool; Utrecht University, Utrecht, The Netherlands, 1999.
(52) Altomare, A.; Burla, M. C.; Camalli, M.; Cascarano, G. L.; Giacovazzo, C.; Guagliardi, A.; Moliterni, A. G. G.; Polidori, G.; Spagna, R. *J. Appl. Crystallogr.* **1999**, *32*, 115.
(53) Sheldrick, G. M. SHELXL-97, Program for Crystal Structure Refinement; University of Göttingen, Germany, 1997.